Kaunas University of Technology

Faculty of Mechanical Engineering and Design

Development of 3D Printed Multi-material Piezoresistive Load Sensor

Master's Final Degree Project

Pratik Pandurang Joshi

Project author

Chief researcher Rolanas Daukševičius

Supervisor

Kaunas, 2023

Kaunas University of Technology

Faculty of Mechanical Engineering and Design

Development of 3D Printed Multi-material Piezoresistive Load Sensor

Master's Final Degree Project

Mechatronics (6211EX017)

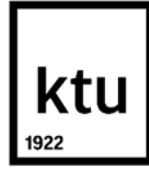**Pratik Pandurang Joshi**

Project author

Chief researcher Rolanas Daukševičius

Supervisor

Lect. Tomas Kuncius

Reviewer

Kaunas, 2023

Kaunas University of Technology

Faculty of Mechanical Engineering and Design

Pratik Pandurang Joshi

Development of 3D Printed Multi-material Piezoresistive Load Sensor

Declaration of Academic Integrity

I confirm the following:

1. I have prepared the final degree project independently and honestly without any violations of the copyrights or other rights of others, following the provisions of the Law on Copyrights and Related Rights of the Republic of Lithuania, the Regulations on the Management and Transfer of Intellectual Property of Kaunas University of Technology (hereinafter – University) and the ethical requirements stipulated by the Code of Academic Ethics of the University;

2. All the data and research results provided in the final degree project are correct and obtained legally; none of the parts of this project are plagiarised from any printed or electronic sources; all the quotations and references provided in the text of the final degree project are indicated in the list of references;

3. I have not paid anyone any monetary funds for the final degree project or the parts thereof unless required by the law;

4. I understand that in the case of any discovery of the fact of dishonesty or violation of any rights of others, the academic penalties will be imposed on me under the procedure applied at the University; I will be expelled from the University and my final degree project can be submitted to the Office of the Ombudsperson for Academic Ethics and Procedures in the examination of a possible violation of academic ethics.

Pratik Pandurang Joshi

Confirmed electronically

ktu
1922

Kaunas University of Technology

Faculty of Mechanical Engineering and Design

Tasks of the Master's final degree project

Given to the student – Pratik Pandurang Joshi

1. Title of the Project

Development of 3D Printed Multi-material Piezoresistive Load Sensor

(In English)

3D spausdinto kelių medžiagų pjezovaržinio apkrovos jutiklio kūrimas

(In Lithuanian)

2. Hypothesis

Multi-material piezoresistive sensor with well-bonded layers of conductive and dielectric polymeric materials can be economically fabricated by using a standard single-extruder 3D printer.

3. Aim and Tasks of the Project

Aim: To develop a polymeric piezoresistive load sensor and its multi-layer components consisting of conductive and soft dielectric materials.

Tasks:

1. To design multi-material piezoresistive load sensor using serpentine conductive component on soft biocompatible layers and select suitable electronics for sensor signal processing.
2. To create a more efficient shear test procedure for multi-material 3D printed parts and evaluate inter-layer bonding strength for the sensor component.
3. To fabricate multi-material load sensor using a low-cost single extruder 3D printer and experimentally determine the piezoresistive sensitivity.
4. To estimate the manufacturing cost of the 3D printed piezoresistive load sensor and compare with other similar sensors.

4. Initial Data of the Project

NA

5. Main Requirements and Conditions

SolidWorks software, Proteus circuit simulator, Prusa i3 MK3 printer, PrusaSlicer 2.5.0 software, Bondtech LGX extruder, Tinius Olsen H25KT UTM, FiloAlfa BioFlex filament, Nylon FX256 filament, ColorFabb XT-CF20 filament

Project author	Pratik Pandurang Joshi		2022.09.26
	(Name, Surname)	*(Signature)*	*(Date)*
Supervisor	Rolanas Daukševičius		2022.09.26
	(Name, Surname)	*(Signature)*	*(Date)*
Head of study field programs	Regita Bendikienė		2022.09.26
	(Name, Surname)	*(Signature)*	*(Date)*

Summary

In this research study, a 3D-printed piezoresistive load sensor was developed. Using SolidWorks modelling software, a piezoresistive load sensor consisting of multi-layered polymeric components, conductive (serpentine structure), and biocompatible substrate materials were modelled. The CAD models were converted to STL files, and those files were sliced using PrusaSlicer to generate g-codes for the Prusa i3 MK3 3D printer. The current study is intended to fill the research gap in order to overcome the difficulties associated with measuring mechanical strength, such as shear, tear, etc. After numerous trials and errors, printing failures, and testing hurdles, a novel shear test procedure using UTM was developed to evaluate interlayer bonding between sensor components. As per the shear testing methodology, the most suitable temperature during printing to obtain greater interlayer bonding was around 230 °C. Subsequently, the multi-material load sensors were redesigned, 3D printed, and tested using UTM. The results for parallel load show an exponential increase in internal resistance from 120 kΩ to 1.8 MΩ when an external force of 0-70 N is applied. On the basis of the experimental results, a suitable circuit with E-CAD was proposed for signal processing of the load sensor. Finally, a concise explanation and evaluation of the cost required for the economical production of the piezoresistive load sensors using a standard single-extrusion 3D printer were provided.

Santrauka

Šiame darbe buvo sukurtas 3D spausdinimo būdu gaminamas pjezovaržinis apkrovos jutiklis. Naudojant SolidWorks programinę įrangą buvo suprojektuotas daugiamedžiaginis apkrovos jutiklis, sudarytas iš elektrai laidžių polimerinio kompozito sluoksnių suformuotų ant biosuderinamo polimerinio dielektrinio pagrindo. Sudaryti SolidWorks modeliai buvo konvertuoti į STL formato modelius, kurie buvo naudojami apkrovos jutiklių maketų spausdinimui naudojant Prusa įrenginį. Daugiasluoksnių bandinių stipruminių savybių nagrinėjimui buvo atlikti įvairūs mechaniniai bandymai šlyties apkrovos ir plėšiamosios apkrovos režimuose. Šiame darbe buvo pasiūlyta daugiamedžiaginių spausdinių tarpsluoksninės sandūros kokybei įvertinti skirta šlyties bandymų metodika. Ji leidžia universalios bandymų mašinos pagalba nustatyti didžiausias šlyties jėgas ir tokiu būdu efektyviai ir greitai įvertinti skirtingų medžiagų sluoksnių susilydymo stiprumą, tam panaudojant suprojektuotus specialios konstrukcijos daugiasluoksnius bandinius, kurie tvirtinami suprojektuotame originalios konstrukcijos, 3D spausdinimo būdu ekonomiškai pagaminamame, laikiklyje. Pasitelkus šią metodiką ir atlikus eksperimentinę šlyties stiprumo analizę buvo nustatyta, kad didžiausias tarpsluoksninio susilydymo stiprumas pasiekiamas kuomet laidūs sluoksniai ant dielektrinio pagrindo spausdinami naudojant maždaug 230 °C ekstruzijos temperatūrą. Atspausdinti apkrovos jutikliai buvo ištirti atlikus pjezovaržinius matavimus tam pasitelkiant universalią bandymų mašiną ir multimetrą. Nustatyta kad didinant apkrovą 0-70 N intervale, atspausdinto jutiklio varža didėja netiesiškai nuo 0,12 MΩ iki 1,8 MΩ. Atlikus ekonominius skaičiavimus buvo nustatytos suprojektuoto apkrovos jutiklio gamybos sąnaudos atsižvelgiant į tai, kad jutiklis realizuojamas standartiniu 3D spausdintuvu turinčiu vieną ekstruderį.

Table of Contents

List of Figures

List of Tables

List of Abbreviations

Abbreviations:

3DP – 3-dimensional printing

ABS – Acrylonitrile Butadiene Styrene

ADC – Analog to digital converter

AM – Additive manufacturing

AMF – AM file

ASTM – American Standard for Testing and Materials

CAD – Computer-aided design

CF – Carbon fibre

CNT – Carbon nanotubes

DC – Direct current

DW – Direct-write

E-3DP – Embedded 3D printing

EVS – Embedded vision system

FDM – Fused deposition modelling

FFF – Fused filament fabrication

GF – Gauge factor

ISO – International Organization for Standardization

MHR – Machine hourly rate

PA – Polyamide

PCB – Printed circuit board

PLA – Polylactic acid

R&D – Research and development

TPU – Thermoplastic polyurethane

UTM – Universal testing machine

Introduction

3D printing has gained great attention for its potential to revolutionize manufacturing techniques within Industry 4.0, allowing faster prototyping, more inventive, and complicated design freedom compared to conventional manufacturing. The combination of biochemical, electrical, electromagnetic, and thermosensitive properties may be integrated into the design of a 3D printed device through the integration of distinct functional components. In recent years, most of the 3D printed sensor research and development has focused on specific fields such as electronics, load, movement, optics, etc. Electronic signals and force detecting units are specifically well-suited for 3D printing, whereas other sensor categories are typically developed by integrating commercial elements into 3D printed structures.

To implement modern 3D printing techniques, it is necessary to reduce the production costs of 3D printed sensing components and increase the number of raw material options, which creates an entrance for the use of material extrusion techniques such as Fused Filament Fabrication (FFF). However, the FFF technique itself has limitations when printing multi-material components with a standard low-cost single-extruder printer. This makes printing difficult, particularly when utilizing multi-material components whose layers are prone to delaminate, which may lead to a decrease in sensor efficiency. On the other hand, there are few research articles with insufficient experimental data available online that discuss the interlayer bonding strength between conductive and soft dielectric filaments when internal resistive changes in conductive materials are taken into account.

Recent availability of biocompatible soft materials for 3D printing has the potential to be one of the most exciting advancements in the evolution of customized wearable technology. The application of a 3D printable electro-conductive filament paved the way for the development of a load sensor that is both cost-effective and customizable using a standard single-extruder 3D printer.

This project aims to develop a polymeric piezoresistive load sensor and its multi-layer components consisting of conductive and soft dielectric materials. In order to achieve the aim, the following tasks are addressed:

1. To design multi-material piezoresistive load sensor using serpentine conductive component on soft biocompatible layers and select suitable electronics for sensor signal processing.
2. To create a more efficient shear test procedure for multi-material 3D printed parts and evaluate inter-layer bonding strength for the sensor component.
3. To fabricate multi-material load sensor using a low-cost single extruder 3D printer and experimentally determine the piezoresistive sensitivity.
4. To estimate the manufacturing cost of the 3D printed piezoresistive load sensor and compare with other similar sensors.

1. Literature review

A sensor is a functional instrument that detects a physical quantity and then transforms to a measurable value. A sensory setup is typically made up of a detector, a processor, and an analog signal to digital converter. The detector identifies the input data and transmits it to the processor. The input data are then enhanced and filtrated inside the processor module applying relevant methods as shown in Figure 1. For increased quality and visualisation, an analog to digital converter can transform the data into a digital output.
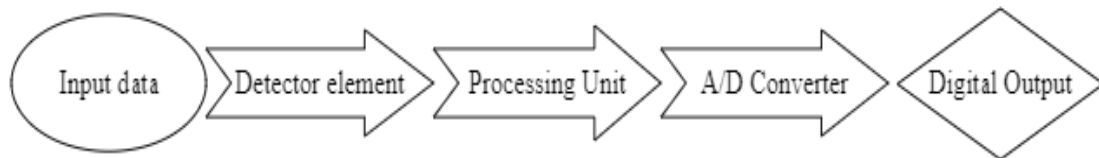
Fig.1. Sensing device fundamentals

Sensors are essential in many fields, including medicine, manufacturing, research, and everyday activities [1]. Sensors can be manufactured by both conversional subtractive manufacturing and novel additive manufacturing techniques. Traditional techniques are effective for mass production, where products are classified by its simpler design as well as the limitation of customization, meaning reduced complexity. Whereas additive manufacturing provides high customization and great level of complexity in a manufactured product. When compared to conventional production procedures, AM offers health benefits because it eliminates rigorous interaction with unpleasant, possibly hazardous workplace environments. Because of the digital ecosystem of the AM production method, digital files may be quickly exchanged and modified on a distribution level. There have recently been several publications covering the use of 3D printing manufacturing processes for efficient electrical components and devices [2]. 3D printing technology is used to manufacture various flexible sensors due to its low processing cost, high fabrication precision, and high production efficiency. Smart device 3D printing is a rapidly expanding field that has applications in smart wearables, prosthetics, and human-machine interaction.

1.1. Overview of new generation sensor and its types

Wearable sensors would be essential for the development of future and stretchable electronics. Wearable sensors for biomedicine have been designed and developed to handle physical measures such as heart rate, temperature, brain movement, and other significant data. Conventional wearable sensing systems are often less adjustable and rely on single-point temperature contact measurements of electrical and mechanical characteristics [3]. With properties such as ultra-high sensitivity, minimal energy consumption, and self-adaptation, the bioinspired sensor system is at the core of modern sensor technology of next-generation sensor development.

1. Piezoresistive sensor - The piezoresistive phenomenon caused by elastic deformation of piezoresistive components is the operating principle of piezoresistive sensors. In other words, the piezoresistive effect modifies the resistance of a component as it is subjected to physical stress. This further results in a relative change of electrons passing forward through the sensor, which also corresponds to a digital output. Most of such devices were also offered with a wide variety of sensitivity characteristics for use in different industry segments. Recent reports indicate that piezoresistive sensors are widely used in biological applications. This research mainly focused on

the implementation of a piezoresistive effect for 3D printed components. Figure 2 represents the current development in new-generation sensor types.
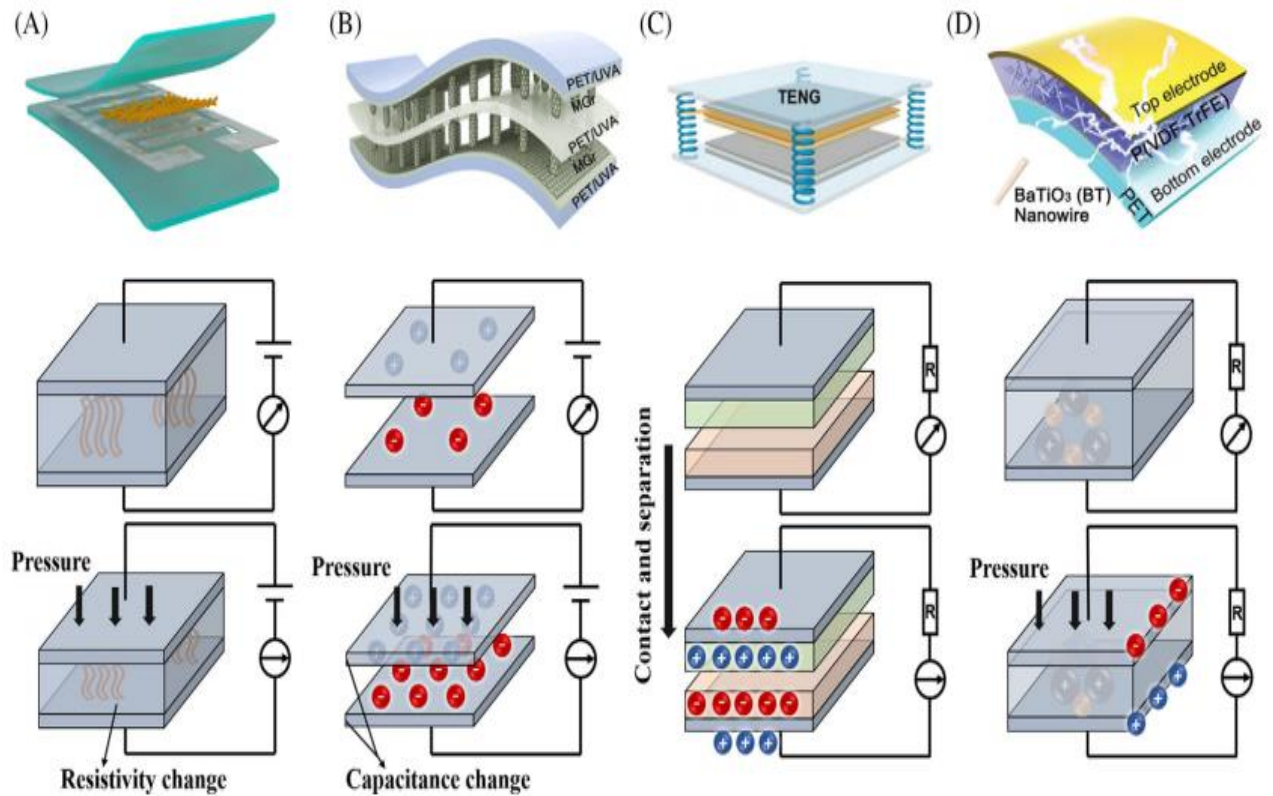
Fig.2. New generation sensor type (a) piezoresistive (b) capacitive (c) triboelectric (d) piezoelectric [4]

2. Capacitive sensor - The capacitance of a parallel plate capacitor can be determined using the formula $C = \varepsilon A /d$, where ε is the dielectric electric constant, and A and d demonstrate the overlap region and the distance between adjacent plates. The standard capacitive sensor is restricted by its size since the fringe effect becomes quite visible when the capacitive sensor's volume is small.
3. Triboelectric sensor - TENGs use the triboelectric phenomenon and electrostatic induction to transfer mechanical force into electrical energy. The electron affinity of the friction layer materials and the structure of the substrate layer are significant aspects influencing the mechanical and electrical characteristics of a triboelectric sensor.
4. Piezoelectric sensor - Piezoelectric sensor capable of converting mechanical load into electrical impulses. When an external stress is applied to an asymmetric crystal in a single axis, the electric polarization develops internally, and charges of opposite polarities are created on two surfaces perpendicular to the polarization direction. As soon as the external force is removed, the crystal reverts to its original state. As the direction of the external force changes, the polarisation of the charge varies. The quantity of charge generated by the crystal is proportional to the magnitude of the external force [4].

1.2. Overview of multi-material 3D printing in sensor development

This subchapter is focused on a discussion of equivalent research conducted in recent years, which primarily focusses on zigzag structured, piezoresistive, and multi-material 3D-printed sensing elements.
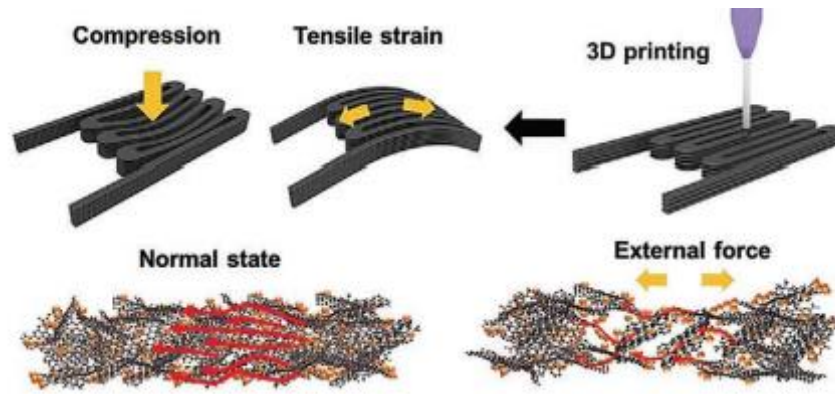
Fig.3. Mechanism of piezoresistivity in 3D printed components [5]

The primary purpose of electronics in the field of 3D printing is to give sensing capability to printed parts. The recent development of piezoresistive sensors uses the principle of a strain gauge. When the electro-conductive material undergoes tension, it elongates and becomes thinner. Since the resistance of any material is directly proportionate to the length, elongation will increase the internal electrical resistance of components. In addition, elongation causes a reduction in cross-sectional area, which in turn reduces the electrical contact points and raises the internal resistance. In some materials, the inherent resistance can also increase as it elongates. Therefore, the relative change in resistance is directly proportionate to the amount of force applied considering that the applied force is within the elastic region of a material [5].

Recent developments of 3D printed piezoresistive sensors include two primary types, the first of which uses a silver-based paste as a conductor and sensor, and the second of which uses conductive filaments.

1.2.1. Silver paste-based sensors

(a)   (b)
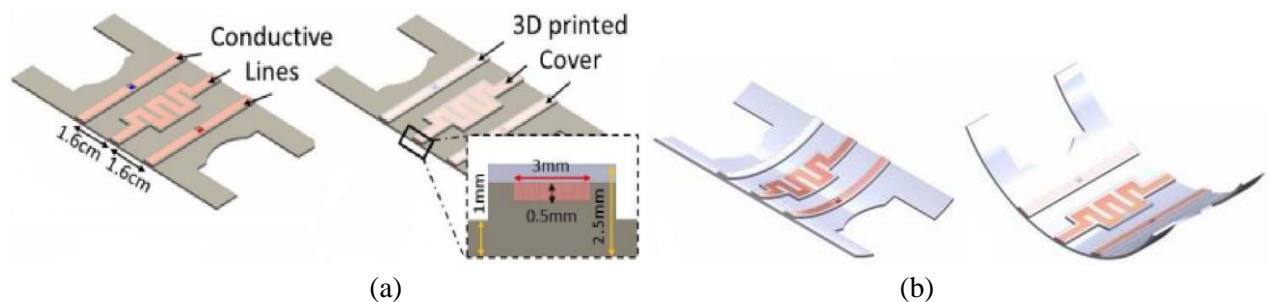
Fig.4. (a) CAD Model of prototype sensory structure (b) bending in X and Y axes [6]

Habib Nassar et al. have developed a prototype flexible sensor structure using silver palladium paste and RS components' clear Glassbend filament. In this method, a 3D printer with a single extruder was modified to 3D print the silver paste on the Galssbend filament substrate. As shown in the Figure 4, the designed structure was tested with X and Y axes bending. The structure demonstrates GF = 1 when the strain was between 3 and 6 percent [6].
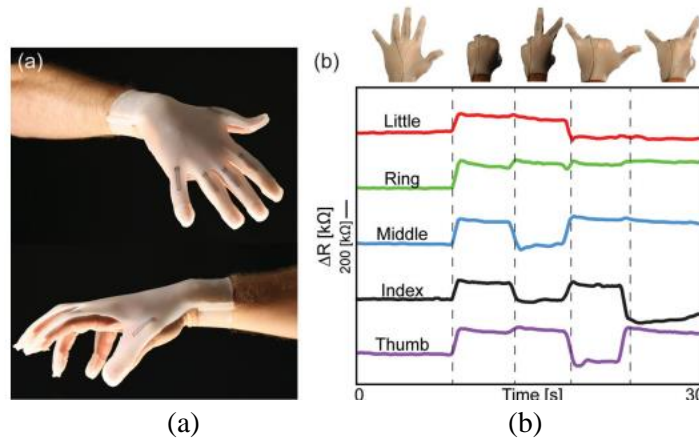
Fig.5. (a) E-3DP manufactured glove with integrated flexible sensory component (b) change in resistance over time in different hand postures [7]

The latest research article has shown that the application of change in resistance in conductive components leads to the development of smart gloves. This study focused mainly on the recent interest in wearable electronics. To enable e-3DP (embedded 3D printing) Joseph T. Muth and colleagues have developed a novel approach as shown in Figure 5, which includes the use of an extruded deposition nozzle to deposit viscoelastic ink in an elastomeric reservoir. The ink acts as a resistive element, and the reservoir acts as a matrix material. As the nozzle moves through the reservoir, a vacuum space is created that must be filled with a capping layer [7].
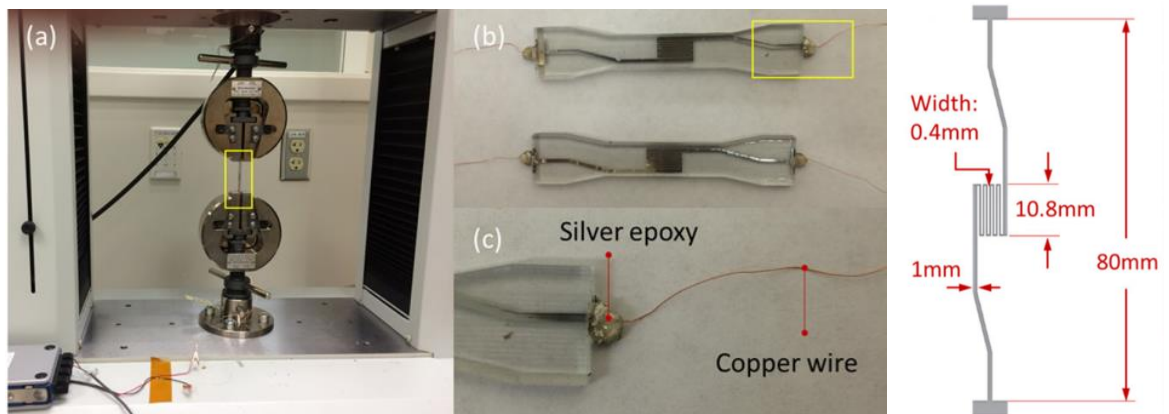
Fig.6. Testing of DW components integrated in a 3D printed part [8]

One of the research studies conducted by Kan Wang in the United States focuses on the implementation of DW components into 3D printed structures using the poly jet 3D printing method. In this study, the test specimen was prepared in the shape of a dog bone, where the gage dimensions were kept as 35 x 10 X 3 mm and 10 nm sized nano silver ink (UTDAg) was embedded as a conductive component. The test specimens were tested using precision UTM and cyclic load applied to obtain a resistance change in the sensory component. This research also proposed the application of such devices in prosthetics, flexible materials for strain measurement [8].

1.2.2. Conductive 3D printable filament-based sensors

Recent research shown in Figure 7 where two sensors with different internal structures have been developed by S. Kouchakzadeh and colleagues, using ABS (Acrylonitrile Butadiene Styrene) + carbon black based Kimya ABS Carbon 3D Filament, 1.75 mm sandwiched between TPU

15

(Thermoplastic polyurethane) based NinjaFlex Filament, 1.75 mm. Compared to the first sensor, the second sensor showed an even more uniform distribution of strain, relative resistance, and gauge factor [9].
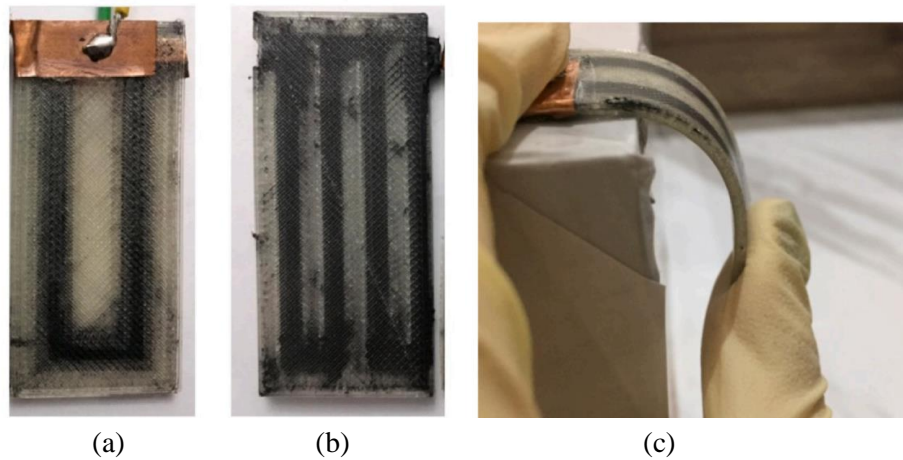
Fig.7. Sensors manufactured by FFF technique (a) sensor 1 along with electrode plate (b) sensor 2 (c) printed sensor 1 after deformation [9]

One research approach involved the use of both conductive and substrate filaments were taken from the same company FiloAlpha3D, Italy. A test specimen was prepared using FiloAlfa PLA (polylactic acid) as a base material and AlfaOhm conductive filament on top of it. The four-point bending test was conducted by Ilaria Mileti and colleagues in 2021 on a printed specimen to check the reproducibility of the 3D printed strain gauge focused on inter-day variation of static performance of PLA material [10].
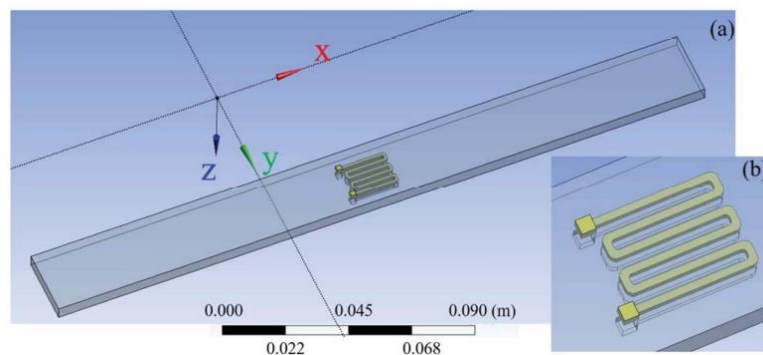
Fig.8. Design of specimen (a) base structure and sensitive gauge (b) embedded sensor on top [10]

In 2018, Khaled Elgenidy et al. performed a method that incorporates commercially available filaments to integrate a sensory component into a flexible structure. This research used a dual extruder 3D printer and NinjaTek's NinjaFlex filament to print flexible parts, and ProtoPasta conductive PLA to print conductive parts of the sensor. The strain sensor and the flexible actuator made up the two components of the sensor actuator, which were welded together as shown in Figure 9. Arduino and pneumatic pressure controllers were utilized to implement the pneumatic supply and obtain the actual bending of the actuator [11].
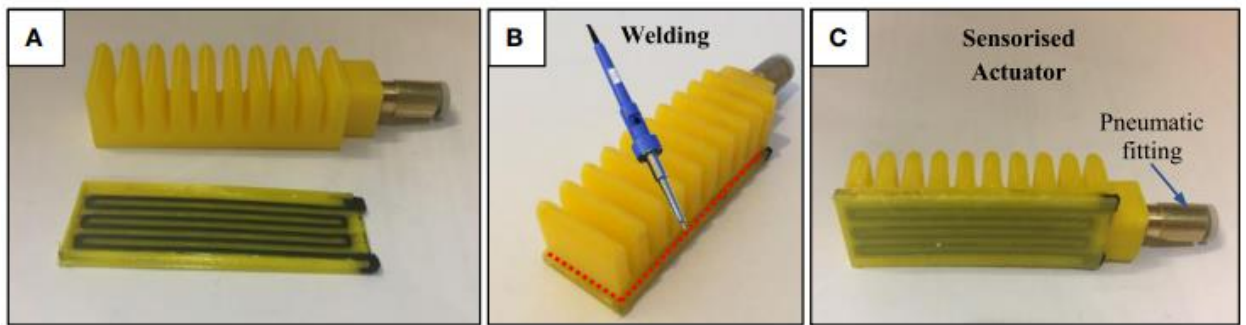
Fig.9. (a) Printed strain gauge and actuator (b) and (c) development of sensorised pneumatic actuator [11]

The sensorised actuator was tested multiple times by applying and removing the pneumatic supply and output data regarding the change in resistance were used to calibrate the actuator with the output measured by the vision system [11].
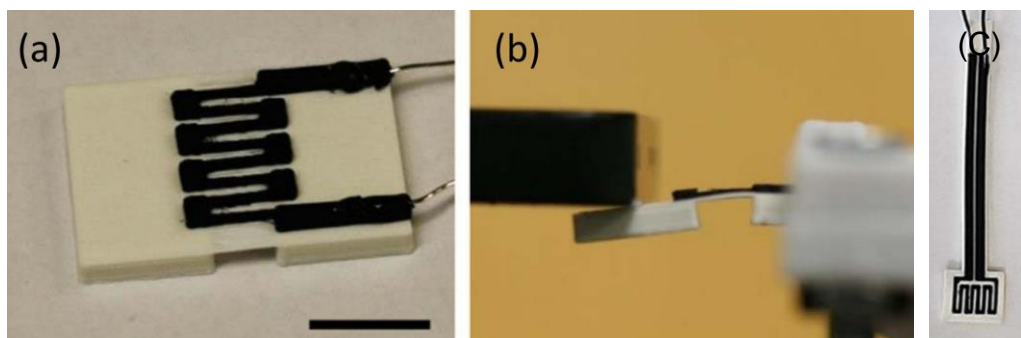
Fig.10. (a) and (b) Piezoresistive sensor placed in the bending load (c) thermoresistive sensor [12]

Similar research conducted by Nathan Lazarus et al. focusses on the piezoresistive and thermoresistive properties of conductive ProtoPasta PLA. The strain sensor was designed with four turns of zigzag patterned conductive filament printed to measure the change in internal resistance when a perpendicular bending load was applied vertically downward with a bending angle limited to ten degrees. In this research four turns were used to increase the surface area of the thermoresistive sensor, and both sensors demonstrate exponentially increasing resistance. Research concluded that the combination of a 3D printed temperature strain sensor with a contact switch could be developed using inexpensive filaments [12].
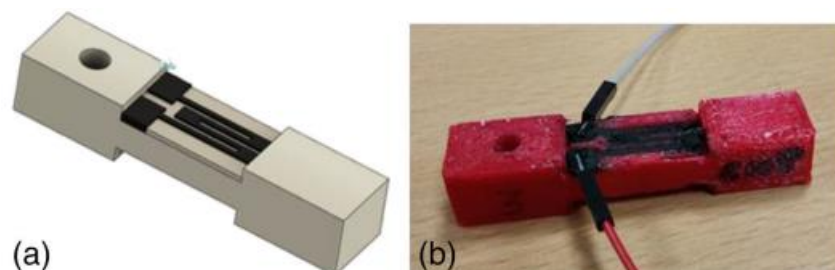
Fig.11. CAD model and actual 3D printed sensor integrated with a strain gauge [13]

Gianni Stano et al. conducted research in 2020 using three commercially available electroconductive filaments: Ninjatek EEL, FiloAlfa AlfaOhm conductive PLA, and Fabbrix® CNT. The research was oriented to the investigation of effect of different printing parameters and different design parameters on the internal resistance and variability of 3D printed strain gauge as shown in figure. In conclusion,

17

printing parameters have a significant impact on resistance, especially the layer height increment, whereas printing orientation has a significant impact on resistance drop. The minimum internal resistance of the strain gauge was achieved by selecting optimal printing parameters. Even resistance is affected by the design parameters, however, there does not appear to be an influence on variations [13].

1.3. Overview of 3D printing filaments for sensor manufacturing

This subsection presents a comprehensive analysis of commercially available 3D printing filaments that could be used as a sensor component as well as a test of a printed component.

1. Analysis of commercial high-strength composite filaments for shear test fixture

   In order to calculate interlayer bonding between conductive and soft dielectric filaments, a novel test was introduced and developed in this research. The shear test requires a high-strength composite filament for the shear test fixture. Following Table 1 shows a commercial high-strength filament.

Table 1. Summary of commercially available high-strength composite filaments

No.	Filament producer, Brand name	Material composition (incl. filler %)	Tensile modulus & strength	Flexural modulus & strength	Disadvantages	Advantages, other features	Ref
1.	Fiberthree F3 PA-CF Pro	PA6 CF (15%)	10.5 GPa & 110 MPa	4.78 GPa & NA	• Hygroscopic • Harden steel nozzle required	• Hard and tough • Low warping effect • Excellent adhesion to epoxy based fibre plates	[14]
2.	ColorFabb XT-CF20	CF (20%)	NA & 76 MPa	6.2 GPa & 110 MPa	• Tendency to overflow • Clumps at nozzle	• Rigid and Durable • Temp resistance up to 80 °C • Excellent availability	[15]
3.	DSM Novamid® ID1030 CF10	PA6/66 CF (10%)	7.63 GPa & NA	NA	• Hygroscopic • Bed adhesion required	• High inter-layer strength • Useful for Medical braces and prosthetics	[16]
4.	LUVOCOM 3F PAHT® CF 9891 BK	PA6 CF (15%)	11.5 GPa & 130 MPa	NA	• Harden steel nozzle required • Dry box required	• Reduced water absorption • Useful for functional prototypes	[17]
5.	BASF Ultrafuse PAHT CF15	CF (15%)	8.4 GPa & 103 MPa	8.26 GPA & 160 MPa	• Poor bridging and overhangs • Risk of Nozzle clogging	• Temp resistance up to 150 °C • Compatible with water-soluble filaments • Good chemical resistance	[18]
6.	Jabil PA 4535 CF	PA6 CF (40%)	10.6 GPa & 88 MPa	5.42 GPa & 118 MPa	• Pre-heating required • Hygroscopic • Ruby-tipped nozzle required	• Increased stiffness and strength • Safe ESD • Useful in Aluminium replacement parts	[19]
7.	XSTRAND™ GF30-PA6	PA6 GF (30%)	7.4 GPa & 102 MPa	6.1 GPa & 170 MPa	• Exhaust ventilation required • Bed adhesion required • Sensitive to Moisture	• Large Operational Temp Range • High wear resistance • High stiffness and strength	[20]
8.	FibreX™ PP+GF30	PP + GF (30%)	6.75 GPa & 65 MPa	5.32 GPa & 85 MPa	• Less availability	• Drying was not required • Less warping • Chemical resistance	[21]

Among the analysed high strength composite filaments, the ColorFabb XT-CF20 filament having 20 present carbon fibres was the most suitable filament for this project due to its dimensional accuracy, high melding strength, higher design stability with less weight and excellent availability in Lithuania with low shipping cost. Therefore, ColorFabb XT-CF20 filament was decided for 3D printing of the shear test fixture.

2. Analysis of commercially available electro-conductive filaments

Whether the sensor is analog or digital, the electrical current-carrying conductor that drives the output single to the receiver and post-processor is vital. In addition, the most recent advancements in piezoresistive 3D-printed sensors demonstrate that the electro-conductive material itself serves as a sensory component and output data driver. Therefore, the optimal design of electro-conductive filaments is essential in sensor development. Table 2 presents a summary of electro-conductive filaments present in European markets.

Table 2. Summary of electroconductive filaments available in European market

Filament brand name	Volume resistivity (Ω-cm)	Surface resistivity (Ω-cm)	Resistance of 10 cm long 1.75 mm filament (Ω)	Composition which causes conductivity	Recomm. nozzle temp. (ºC)	Tensile strength (MPa)	Young's modulus (MPa)	Ref
Proto-pasta conductive PLA	15	30 (Along layer) / 115 (Perpendicular to layer)	2000-3000	Carbon black / Polymer	215	NA	NA	[22]
FiloAlfa AlfaOhm conductive PLA	15	15 (Along layer) / 20 (Perpendicular to layer)	NA	PLA + Carbon nano tubes	190-210	25	1550	[23]
FIBERFORCE Nylforce conductive PLA	10^3	NA	750	Biopolymer compound + Carbon nanotubes	215	30	1550	[24]
Ninjatek EEL	1.5×10^3	NA	1500	Carbon Black + Silica, cristobalite	220 - 230	12	NA	[25]

Despite the slightly higher resistance of 10 cm ProtoPasta conductive PLA filament compared to others, it was decided to use ProtoPasta conductive PLA because of its low cost, ready availability in Lithuania, volume resistivity, and strong interlayer bonding with other substrate filaments, which increase the sensor's efficiency.

3. Review of flexible filaments available in the European market

Table 3. Summary of a commercially available flexible filament.

Brand name, Filament	Shore hardness	Recommended Printing Temperature (ºC)	Density (g/cm^3)	Tensile strength (MPa)	Ref
	Testing method		Testing method	Testing method	
Raise3D Premium TPU-95A	95 Shore A	255	1.24	29.3	[26]
	ISO 7619		ISO 1183	ISO 37	
FiloAlfa BioFlex	27 Shore D	210 – 230	1.09	35	[27]
	ASTM D2240		ASTM D792	ASTM D790	
BASF Ultrafuse TPU 85A	90 Shore A, 37 Shore D	200-220	1.08	NA	[28]
	ISO 7619-1		ISO 1183-1		
KIMYA TPU-92A	92 Shore A	210	1.16	90	[29]
	ISO 868		ISO 1183-1	ISO 37/2/500	
BCN3D TPU 98A	98 Shore A	220	1.16	150	[30]
	ISO 7619-1		ISO 1183	ISO 527	

Table 3 shows a commercially available flexible filament that could be used as a substrate for sensor development. Most electroconductive filaments are rigid and brittle, making them unsuitable for direct use with any type of load; in other words, the possibility of failure is very high. To provide flexibility, commercially available flexible filaments composed of copolyesters or a material with equivalent dielectric properties could be used as a substrate. Amongst the analysed flexible filaments, BioFlex filament by FiloAlfa, Italy was decided to use considering the availability, cost of filaments, biocompatibility, and safety of operator. The BioFlex filament was also certified with several important biocompatible tests, including in vitro cytotoxicity (ISO 10993-5:2009), intracutaneous reactivity (ISO 10993-10:2010), hemolysis test (ISO 10993-4:2002/Amd 1:2006), systemic injection test (ISO 10993-11:2006). Therefore, the BioFlex filament is safe for contact and no hand or skin protection is required [27].

2. Bonding strength measurement for 3D printed sensor components

This chapter of the project focusses on mechanical property measurements of 3D-printed sensor components. To create a fully functional sensor using FFF, the sensor components must have adequate bonding between each layer, including homogenous bonding for flexible filament layers and bonding between flexible and conductive layers. Despite the increasing variety of 3D printers and filaments used for FFF printing, there are currently no standardised structural examination methods designed specifically for FFF-printed components. Thus, conventional testing equipment and a modified testing technique could be used to determine the interlayer bonding strength of multi-material components.

Tinius Olsen H25KT
UTM

Force Signal

ADLINK EOS-1200
Embedded Vision System

Output Data

Monitor
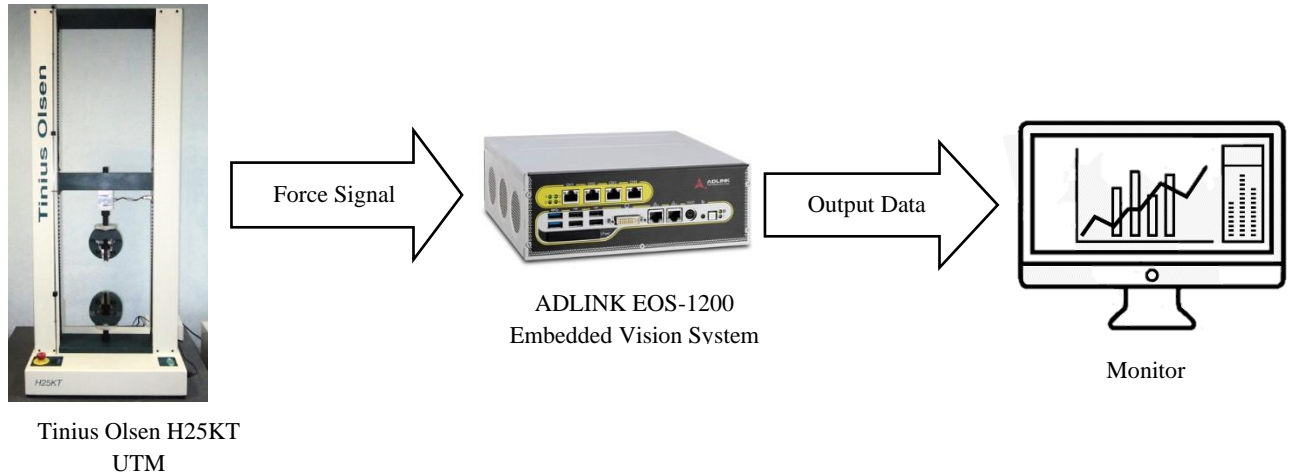
Fig.12. Used UTM to measure bonding strength [31]

The Tinius Olsen H25KT UTM with a 25KN load cell was used throughout this research study. The load cell captures the reaction force value and transmits it to the ADLINK EOS-1200 embedded vision system. EVS converts load signals into output signals that are displayed in the software Tinius Olsen Horizon. The Horizon software can export data points to Microsoft Excel files for further processing.

2.1. Tensile test methodology for 3D printed components

Planned preliminary evaluation of the interfacial bonding between the substrate layer and the conductive layer utilizing conventional tensile method and universal testing machine (UTM). In the initial phase, a simple 3D CAD model was created using the software SolidWorks, with a 10 mm x 10 mm cross-sectional area of the components in contact.
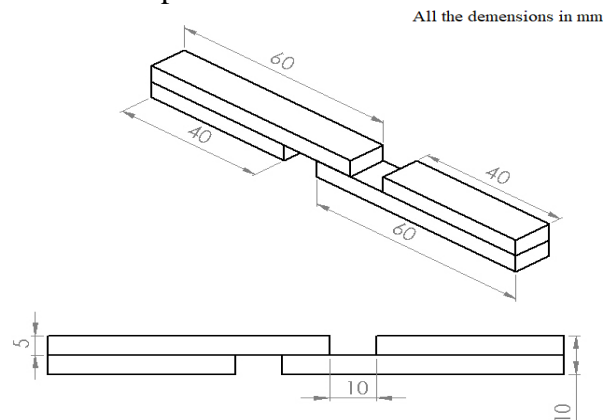
Fig.13. 3D CAD model of the test element for tensile testing

PrusaSlicer 5.0 was used to slice this model with 100 percent infill, and G-codes were generated. The test component was 3D printed using a Prusa i3 MK3 printer equipped with a Bondtech LGX extruder and a 0.4 mm diameter nozzle. Prusa PLA filament was utilised in the experiment to determine the reliability of the test methodology and to prevent failure with costly filaments. PLA filament was also used as a support material for the structure and those supports had to be removed manually after priting.

Fig.14. Captured photos of tensile testing under load condition and deformed components

By analysing the tensile test methodology, it was determined that the force values obtained did not represent the true stress; rather, they represent a mixture of shear, bending and tensile stresses, and the gap between filaments was the underlying cause. Such an assessment method would not be appropriate for measuring the bonding strength of highly flexible filaments.
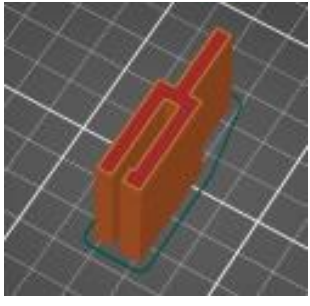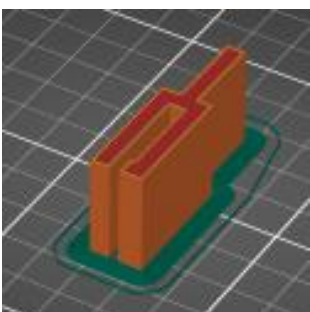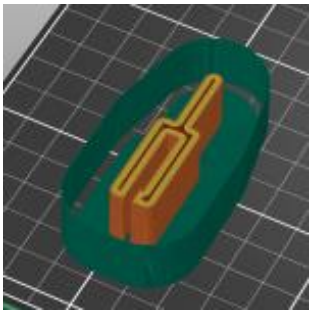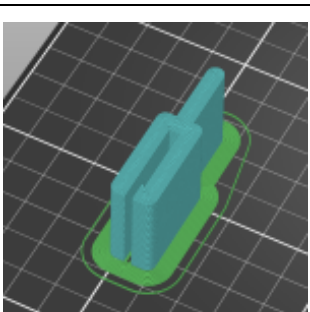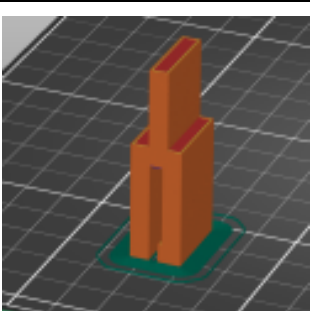
2.2. Shear strength measurement for 3D printed components

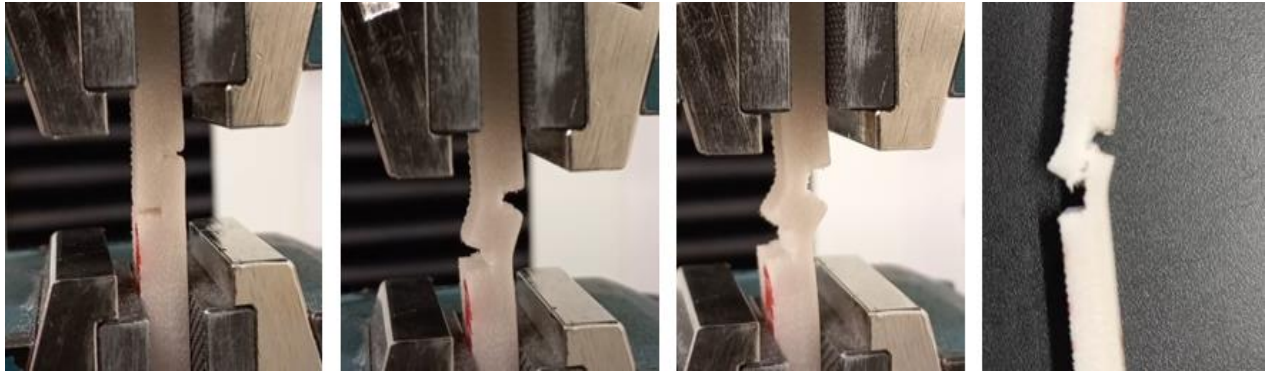To overcome the limitations of the tensile test, a novel method for measuring shear strength has been developed. For this method, the primary objective was to create a universal shear test fixture that can be used to measure practically all specimens and provides immediate shear strength comparisons for any multi-material component. The design of the assembly-free fixture was inspired by the design of a tuning fork. When considering proper clamping of the fixture to the upper clamper of the UTM, the length of the upper neck of the shear fixture is a minimum of 20mm for all designs. One of the fixture's forks was designed with a sharp edge at its end, which was used to shear off the conductive ridges off the substrate filament.

2.2.1. Printing challenges for printing with Nylon filament

The durability and hardness of nylon filaments are widely recognised. It has a high mechanical strength and minimal deflection. Nylon is resistant to bending and fracturing, and its chemical resistance allows for additional industrial applications. Nylon FX256 by Fillamentum additive polymers was selected initially due to its low cost and ready availability in Lithuanian market. However, this showed a significant challenge for the 3D printing of fixture with less accurate dimensions. The primary issue was caused by the bonding between the first layer of nylon and the magnetic bed plate of the Prusa i3 MK3 printer, after finishing 40-50 percent of the print, the print began warping. Printing-related shrinkage of the elastomer was the primary factor of warping (the elastomer expands slightly when melting). However, as it cools, it shrinks, causing the tiny corner to lift up (and sometimes a complete detachment of parts from the hotbed). After forty to fifty percent of the print had been completed, warping began even though the manufacturer's recommended printing parameters had been followed.

Table 4. Brief information about 3D printing of the shear fixture with Nylon FX256 filament

Iteration Number	Sliced fixture STL file with PrusaSlicer software	Actual Picture of 3D Printed fixture	3D printing parameters and key features (Using feedback from previous print)
First time of 3D printing			• Horizontal position on 3D printing bed • Brass nozzle of 0.8 mm used • First layer height of 0.2 mm • Layer height of 0.3 mm DRAFT • Heated bed temperature : 80 °C • Printing speed of perimeter : 70 mm/s • Printing speed of Infill : 100 mm/s • Printing temperature of the first layer : 240 °C • Printing temperature of other layers : 235 °C • Object detached from bed after 64% of print
Second time of printing			• Printing speed of perimeter : 15 mm/s • Printing speed of Infill : 20 mm/s • First layer height : 0.2 mm • Layer height : 0.15 mm QUALITY • Heated bed temperature : 80 °C • Printing temperature of the first layer : 245 °C • Printing temperature of other layers : 240 °C • Brim : width 5 mm, Outer brim only • Infill angle : 90° • Other parameters were same as 1st Iteration
Third time of printing			• Redesigned fixture with curve corners • Applied adhesive spray on a heated bed • Brim : width 10 mm, Outer brim only • Perimeter width : 5 lines • Heated bed temperature : 90 °C • Printing temperature of the first layer : 250 °C • Printing temperature of other layers : 245 °C • Skirt height : 133 layers • Infill density to 90% and Gyroid infill • Other parameters were same as 2nd Iteration
Fourth time of printing			• First layer with Prusa PLA (removed in post processing) and changed filament to print other layers with Nylon FX256 • Applied glue to a printed bed • Brim : width 5 mm and skirt • Nozzle changed to 0.4 mm Brass • Heated bed temperature : 80 °C • Printing temperature of the first layer : 220 °C • Printing temperature of other layers : 245 °C • Other parameters were same as 3rd Iteration
Fifth time of printing			• Changed orientation on a heated bed • Removed curve corners to avoid supports • Brim : width 5 mm, outer and inner brim • Nozzle changed to 0.4 mm Brass • Perimeter width : 2 lines • Infill density to 100% and rectilinear infill • Printing temperature of the first layer : 260 °C • Printing temperature of other layers : 250 °C • Heated bed temperature : 100 °C • Other parameters were same as 4th Iteration

To overcome the difficulties during printing, a positive iterative process was implemented, and changes were made to the CAD design and printing parameters, which had the effect of reducing the warping problem. Table 2 provides a comprehensive explanation of all five printing variations. To overcome these challenges, an iterative process was implemented, and the CAD design and printing parameters were modified, which had the effect of reducing the warping issue. During the first printing attempt, the fixture was positioned horizontally on the bed, a nozzle with a diameter of 0.8 mm was used in, and the printing speed of the 3D printer was 45 mm/s, which was relatively fast, resulting in the fixture detaching completely when 63 percent of the printing was complete. For the second printing, the speed was reduced to 15 mm/s, resulting in a significant reduction in fixture warping, although the fixture corners still warped. The edges of the fixture were redesigned to be rounded for the third printing, but that had no significant effect. For the fourth printing, a nozzle with a diameter of 0.4 mm and a brim of 10 mm was used, resulting in higher-quality prints but with some warping. It was decided to eliminate the fixture's curved edges during the fifth time printing a change of alignment to vertical alignment. Even the fifth print contained the same flaws.

2.2.2. Printing of shear test fixture with ColorFabb XT-CF20 filament
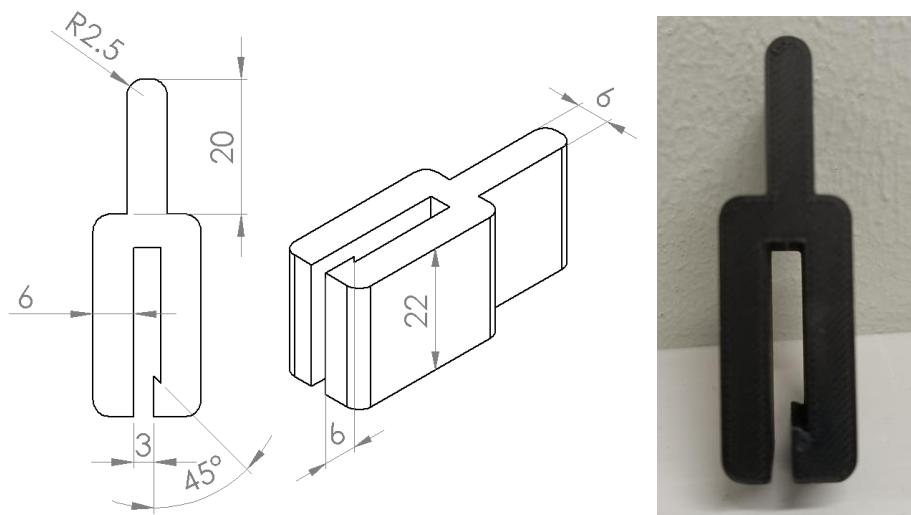
Fig.15. CAD design of shear test fixture and actual 3D printed fixture with XT-CF filament

To resolve printing issues during the shear test fixture, it has been decided to replace the filament with one that contains carbon fibre composites. On the basis of the low cost and availability on the Lithuanian market, a decision has been made. Using ColorFabb's Amphora copolyester-based XT-CF20 filament (containing 20% carbon fibre) to print fixtures increased the dimensional stability and reduced the weight of the fixtures.

2.2.3. Design of shear test specimens with ridges

After selecting the desired dimensions for the shear test fixture and printing it successfully with the XT-CF20 filament, the second essential objective of the shear test was to standardise the optimal design for the test specimens. Multiple factors were considered for multi-material 3D printing, including the cost of filaments and the minimum surface area required to achieve comparable results. In the initial stage of the design of shear test specimens, 10 ridges were used to achieve comparable results. The following Figure 16 shows the CAD design of shear test specimens with ridges.
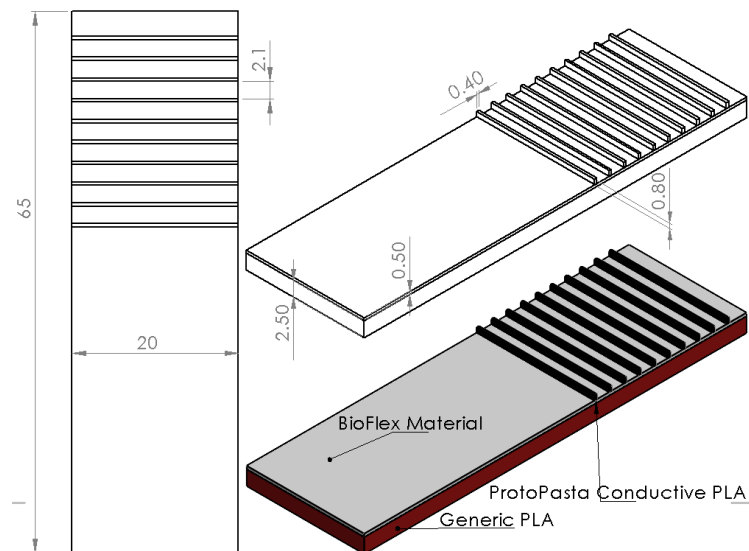
Fig.16. CAD design of shear test specimens with ten ridges

The test specimens were also 3 mm thick, with the base layer 2.5 mm thick and printed on a heated bed using generic PLA material (shown in the figure with red colour). The base layer was helpful in giving the specimens more strength and in reducing the use of an expensive flexible layer. BioFlex filament was used to print the second layer (shown in white). Conductive PLA was used to print the ridges, which are shown in black colour.

2.2.4. Preliminary experimental setup of the shear test and the challenges faced during test

After finalizing the design dimensions as well as successful printing of the shear test fixture and the shear test specimens, shear test was performed with Tinius Olsen H25KT UTM. For this shear test, a 25 kN load cell was used (test setup shown in Figure 17). In total, four specimens have been printed to justify the validation of the shear test methodology.
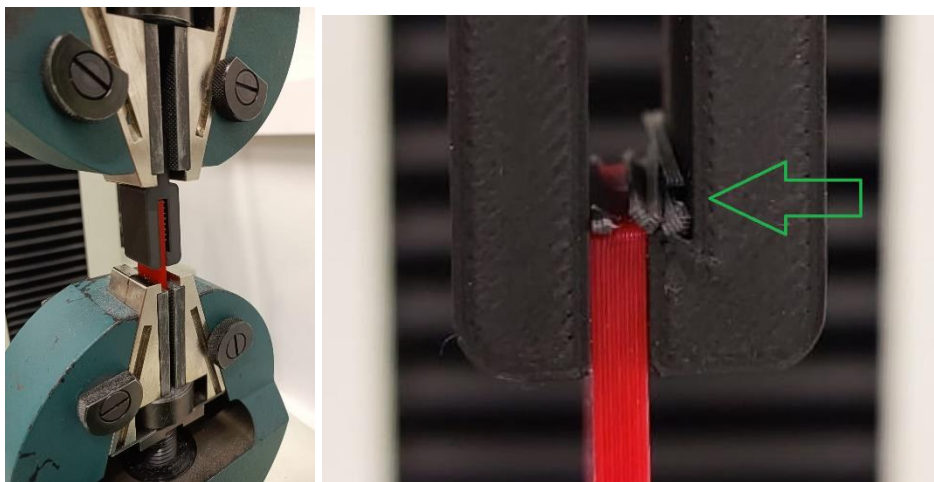
Fig.17. Shear test setup and captured photo of ridges stacking after shearing off

The following Figure 18 shows a graphical representation of the results of the preliminary shear test. The results from the test were inaccurate and the ridges got stuck between the gap of shearing edge, which further leads to an increase in frictional noise.
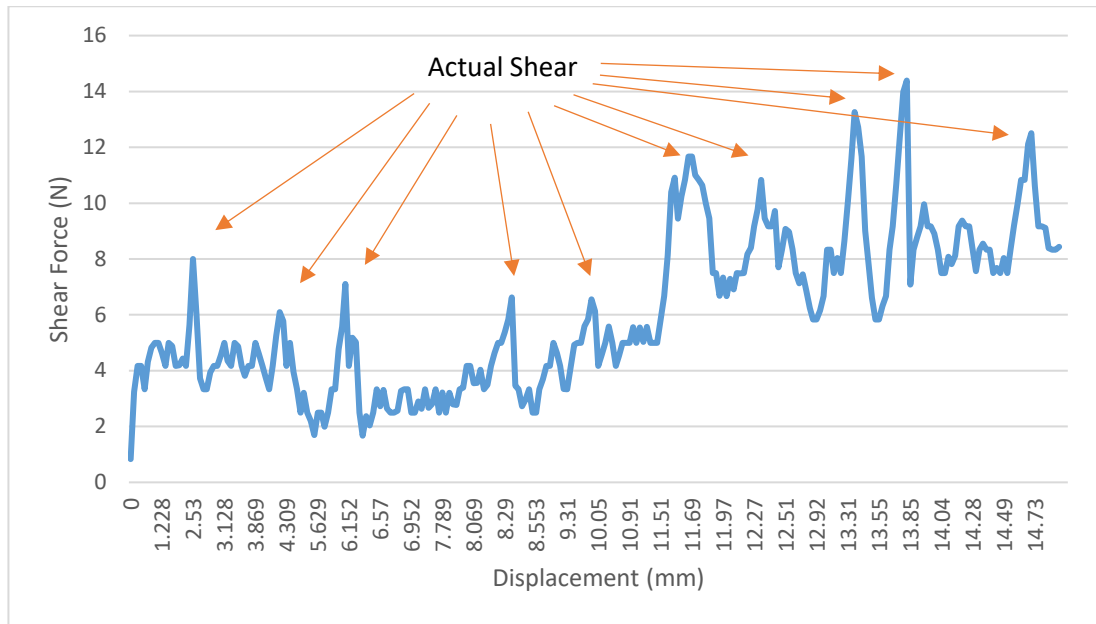
Fig.18. Experimental result of sharing force from preliminary shear test

The results of a preliminary shear test were not satisfactory, due to the following possible reasons.

 – The first and important reason was that the force required to shear off a single ridge was less than 0.1% of the load cell capacity, so the results show high frictional noise force values. Additionally, there could be microlevel printing defects of the 3D printer, such as bed levelling defects, extruder defects which cause large friction.
 – The ridge height was only 0.8 mm long and due to the compressibility of BioFlex filament, a few ridges got stuck in the gap between the shearing edge of the fixture and specimen, after shearing off from its position.
 – The fixture has very less space for ridges after shearing off from its position, which further causes the staking of ridges after shear. After stacking of 4-5 ridges, those ridges hit the adjacent ridge before shearing edge of the fixture, so the output force values continued to increase incorrectly.
 – Two more test specimens were printed with 2.9 mm thickness to reduce frictional noise, but this leads to the expansion of gap between the shearing edge and the test specimen. That results in an almost negligible reduction in frictional values, but more ridges got stuck in that gap.

To overcome these challenges, after analysing the experimental failure of the shear test methodology, changes were made in the design of the fixture as well as specimens.

2.2.5. Redevelopment of shear test fixture

During this part of the research, design of the shear test fixture as well as specimens were changed. After detailed investigation of the failure caused, the shear test fixture was designed in such a way that, after shearing off, the ridges should fall inside the pocket of the fixture. Following Figure 19 shows the CAD design of the redeveloped shear test fixture and the actual printed fixture. Fixture thickness was increased from 6 to 10 mm, resulting in a stiffer design. The fixture can now support ridges with longer heights due to the increased space between the two forks.
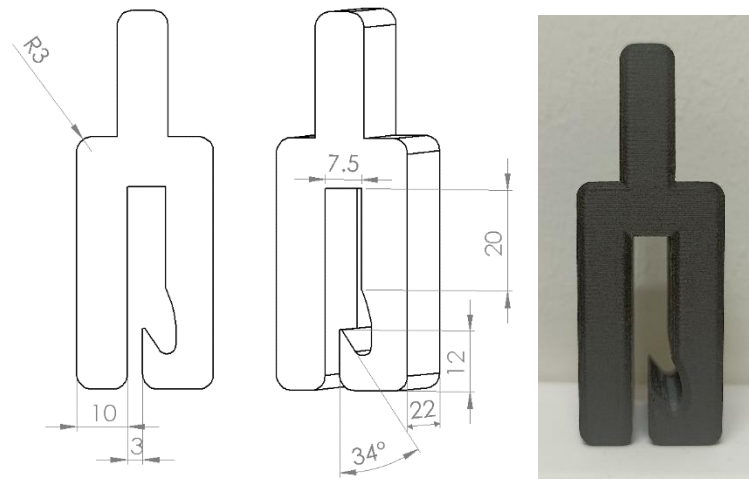
Fig.19. Redesigning of shear test fixture and actual 3D printed fixture

The following Table 5 details the specific printing process parameters for the newly designed fixture. According to the manufacturer's recommendations, the XT-CF20 filament was placed in a dryer for eight hours prior to printing the redesigned shear test fixture.

Table 5. Details of printing process parameters for the redeveloped shear test fixture

3D printing specification	Value, description
Filaments used for 3D printing of fixture	ColorFabb 20% Carbon fiber XT-CF20
3D printer	Prusa i3 MK3
Printer chamber	Open
Extruder	Bondtech LGX
Nozzle diameter	0.4 mm
Extrusion temperature	250 ºC
Build plate temperature	70 ºC
Printing speed	15 mm/s
Infill density	100%

During this stage of the research, the shear test specimens were also redesigned. The number of ridges was reduced from ten to three, but their height was increased to 4 mm. This design was used to print two additional specimens that were tested using UTM to determine the conformity of the test results.
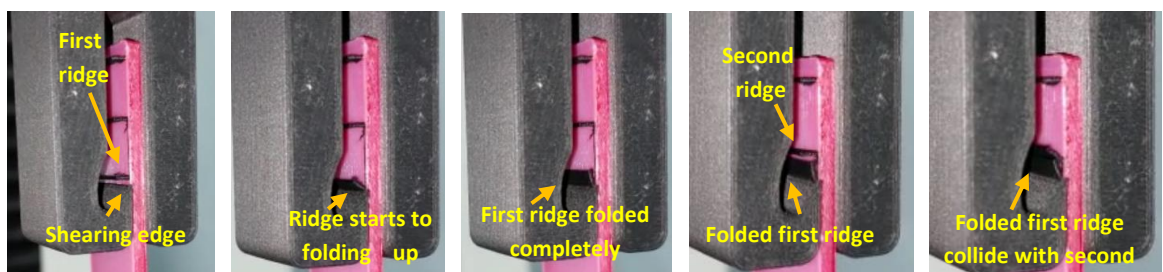
Fig.20. Captured photos when ridges collide with subsequent ridges

Then again, these tests produced unsatisfactory results. Figure 20 captures the actual difficulty encountered during testing. Once the first ridge of the test specimen was sheared off by the shearing edge of the test fixture, it began to fold upward rather than falling into the fixture's pocket. During

testing, the first ridge of the test specimen emerges toward the second, causing the first ridge to collide with the second ridge. The first ridge collided before the shearing edge reached the second ridge, resulting in an incorrect output of the shearing force. After this collision, the second ridge folded and emerged in the direction of the third ridge, and the same collision occurred again in place of the third ridge. Both test specimens produced identical results so, after multiple failures of the shear test methodology and detailed investigation of failures, it was determined that the lack of strength in a single ridge caused inaccurate results, which paved the way for the change of specimen format.

2.2.6. Design of shear test specimens with pillars

When analysing the difficulties experienced in previous tests, the decision was made to alter the specimen format. Instead of a single ridge that does not have any support from the adjacent track, pillars were designed. Initially, two specimens with dimensions of two pillars 2 x 2 x 2 mm, two pillars 3 x 3 x 3 mm, and two pillars 4 x 4 x 4 mm were printed and were reviewed the test results. After printing a trial of test specimens with a Prusa i3 MK3 printer, 2 X 2 X 2 mm pillars had shown insufficient dimensional stability, and the shear force value to shear off a single pillar was quite low during testing (around 15 N). Considering the frictional noise and a 25 KN load cell, the smallest acceptable design dimensions of 3 x 3 x 3 mm pillars was finalised. Taking into account the dimensions of base layer and substrate layer, 5 pillars were placed on one specimen.
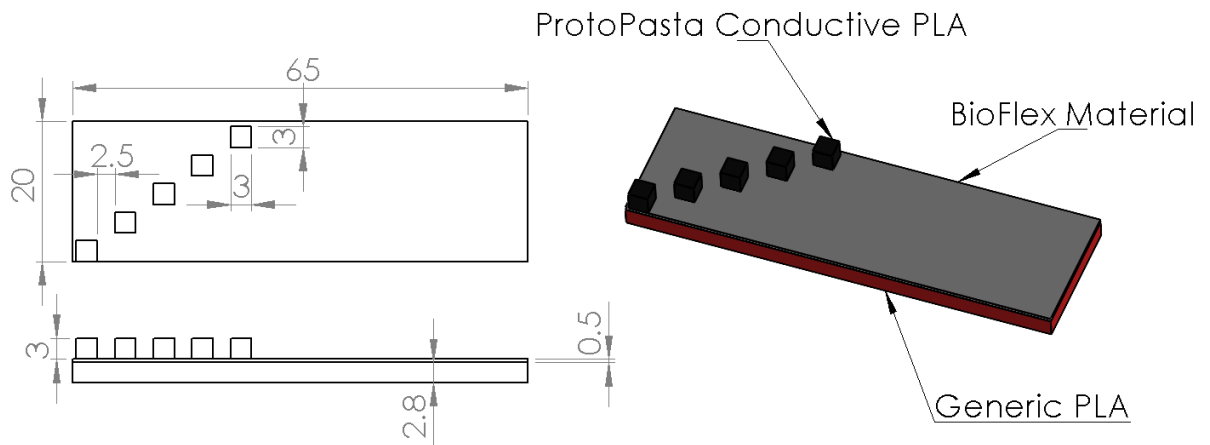
Fig.21. Redesigning of shear test specimens with pillars

For the design of shear test specimens with pillars, the dimensions of base layer and substrate layer were kept as in previous specimens. The length of the specimen was 65 mm, and the breadth was 20 mm. The thickness of the base layer was 2.8 mm and base layer was printed with generic PLA. The thickness of substrate layer was 0.5 mm, and it was printed with BioFlex material. On top of BioFlex material, five pillars of 3 X 3 X 3 mm were printed diagonally as shown in Figure 21.

Using these dimensions, ten specimens were printed and tested using UTM, the selected nozzle temperature while printing pillars on the substrate layer with a step of 5 °C, starting from 215 °C to 235 °C. (Because of the recommended printing temperature by the manufacturer lies in that range). Two specimens for each temperature were printed at the same time on a bed to get the most suitable printing range. However, one specimen of 215 °C and one of 220 °C printing temperature were damaged by the printer nozzle and removed by the printer itself. The primary reason for that was

some wear and tear on the heated bed, but a simple change of position on bed solved the problem and the following specimens were printed correctly as per the requirements of project.
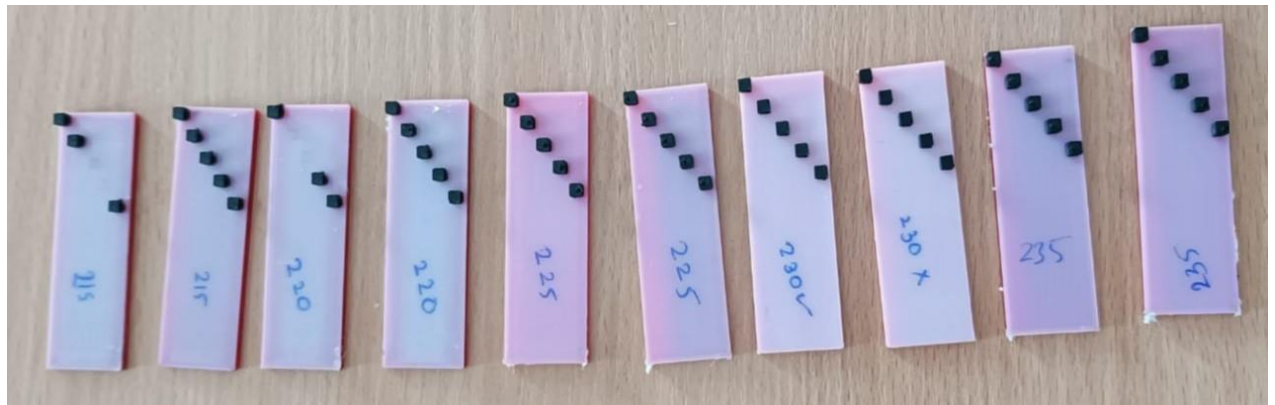
Fig.22. Printed test specimens with a difference in nozzle temperature of 5 °C

An identical shear tests were conducted on all ten specimens, as shown in figure. While 3D printing of these ten specimens, printing speed for the initial five layers was kept constant at 10 mm/s, later for the infill of base layer printing speed increased to 50 mm/s, and it again reduced to 10 mm/s for the substrate layer of BioFlex material and pillars. Two lines of perimeter were applied for the printing of pillars, which results in better stability of the printed pillars.

2.2.7. Results and discussion for shear test methodology

The experimental results show the graphical representation of the shear force (N) required to remove a single pillar from its position.
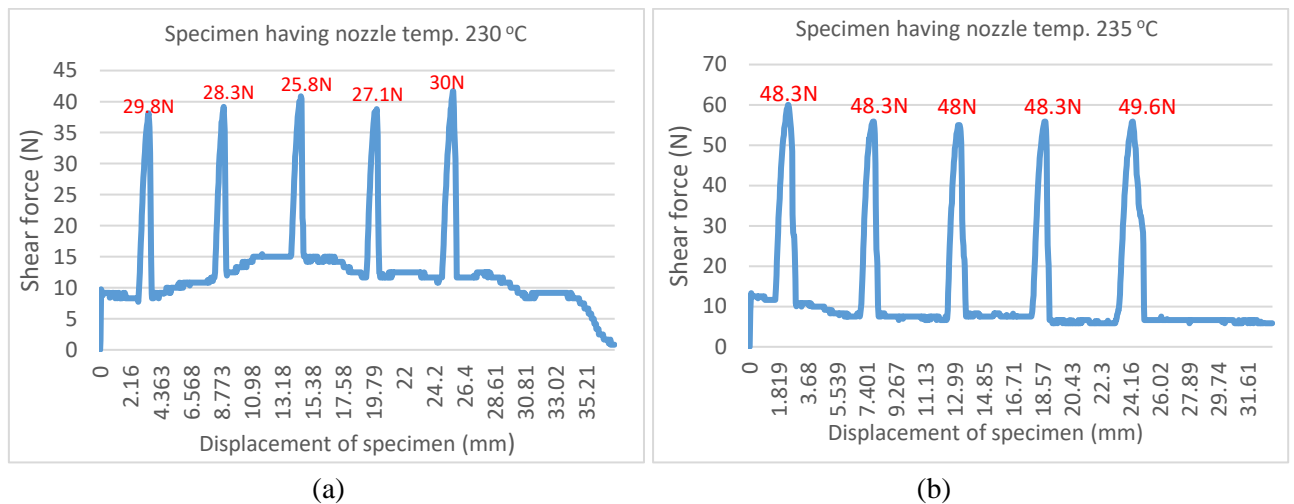
Fig.23. (a) Experimental results of shearing force for a specimen with nozzle temp. 230 °C (b)experimental result of shearing force for a specimen with nozzle temp. 235 °C

Both graphs exhibit significantly larger peaks than previous results. Each peak shows the shear force required to remove one pillar of ProtoPasta conductive PLA from the substrate of BioFlex filament. Values in red represent the shear force after neglecting friction force. Amongst all ten specimens, the specimen graph shown in Figure 23 has excellent repeatability, compared to all other specimens, with temperatures below 230 °C showing a greater coefficient of variation.
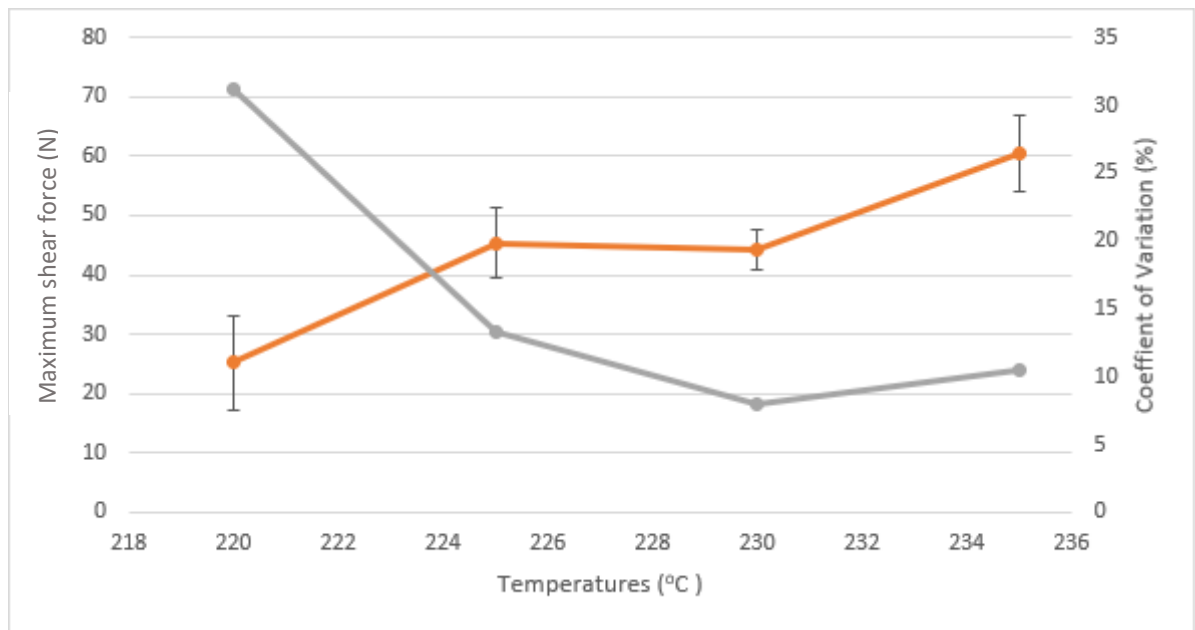
Fig.24. Graphical representation of the maximum shear force required for individual printing temperature and coefficient of variation

To gain a better understanding of the temperature range, which is the most suitable temperature for printing, a graph was plotted for temperature range from 220 °C to 235 °C. Maximum shear force (N) with standard deviation as an error bar on the first y axis vs temperature (°C) on the x axis and coefficient of variation (%) on the second y axis. The graph demonstrates that printing temperature plays a crucial role in the interlayer bonding strength of multi-material 3D printing. As the printing temperature increases within the manufacturer's specified range, the amount of force required to remove the pillars increases, while the coefficient of variation decreases. In conclusion, temperatures around 230 degrees celsius, which is also the manufacturer's maximum permissible temperature, show considerably greater strength than other temperatures. The shear strength value for the printing temperature was calculated as 5 MPa for 3 X 3 X 3 mm pillars. No similar research data was found to compare the shearing force required to shear of ProtoPasta conductive PLA on top of BioFlex substrate filament.

2.3. Trouser tear test methodology for 3D printed components

Numerous process parameters have a considerable influence on the mechanical properties as well as interlayer bonding of FFF 3D printed products, which further restricts structural applications. To evaluate the quality of interlayer bonding, the trouser tear test has been conducted based on ASTM D1938-14 standard method. For the preparation of test specimens, a hollow square-shaped box with a single wall thickness of 0.5 mm was printed with dimensions 80 mm X 80 mm X 30 mm. Both ends of each wall were trimmed, and a rectangular element of 70 mm X 25 mm was prepared. (Bottom 5 mm from the base plate was also neglected due to changes in crystallinity between layers nearer to the heating bed). The pre-crack has been made using a sharp knife and uniaxial load applied with the help of UTM. The following figures represent the experimental methodology for the trouser tear test.
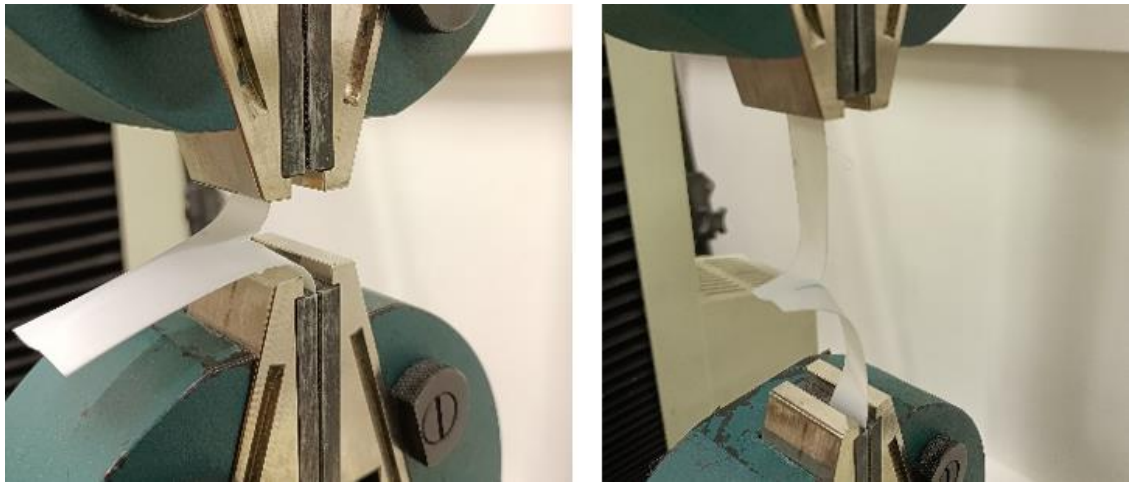
Fig.25. Trouser tear test experimental setup

The interlayer resistance force (F) ranges from 4 to 5 N, when the pulling rate of UTM was 50 mm / min. By getting precise value of width of weld (W_t), Tear strength calculated as $T = \dfrac{2F}{Wt}$, … (1)
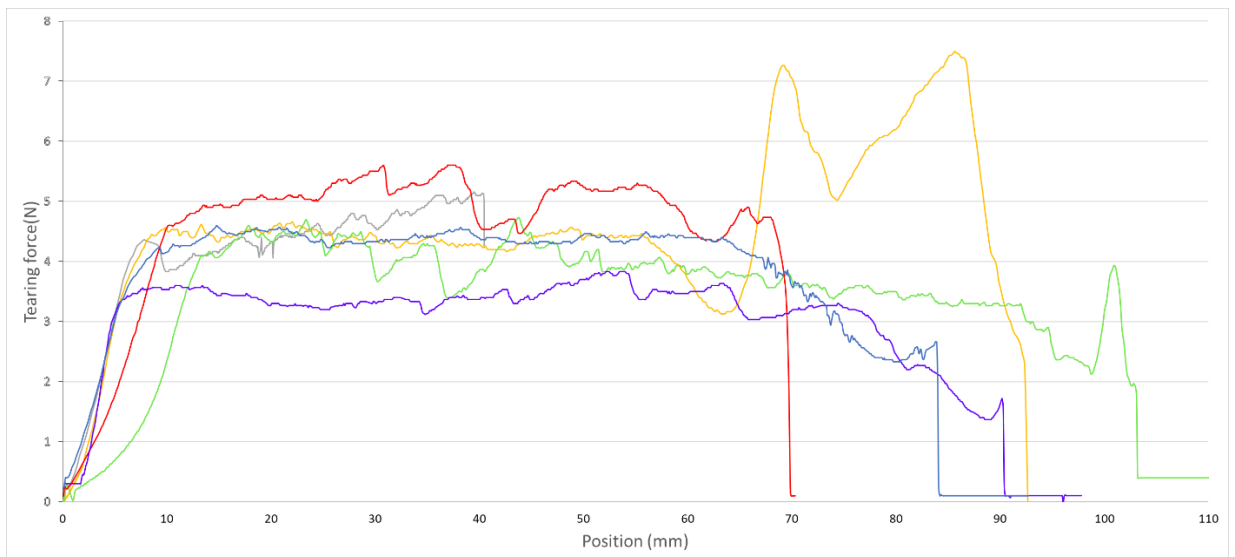
Fig.26. Experimental representation of results from trouser tear test

The results depicted the required tearing force (N) versus the position of the specimen (mm). This test determined that all specimens exhibit a steady increase in the beginning of tearing. Then, as the pulling continues to propagate at a constant rate, the specimens clearly exhibit a stable force range. All specimens showed a substantial increase in tearing force just before the specimen completely teared off, due to tensile elongation at the end. In one of the specimens (shown in yellow colour), the tearing force increases enormously due to the track change at the end of specimen. The track change resulted in two distinct cracks whose tensile elongation values were also added, resulting in a higher tearing force value than other specimens. There was no recent research article found to compare the results of similar filament trouser tests for BioFlex filament.

3. Determination of piezoresistive sensitivity

After the calculation of the mechanical strength properties, this part of the research focusses on the electrical properties of the lead sensor. The load sensor has been developed using the piezoresistive properties of materials. The piezoresistive material shows a change in internal resistance when an external force is applied to it. One of the examples of these materials is 'strain gauge' which shows the deformation in the length of strips. If a strip of an electrical conductor is stretched to its elastic limit, it will become slimmer and longer, leading to a rise in the resistance value. The change in resistance is directly proportional to the amount of force applied. Greater forces can result in a greater resistance change but can permanently deform the strain gauge and/or conductors. In order to prevent damage to the strain gauge, the resistance change measurement must be extremely precise, even for minimal changes.

3.1. Preliminary design of multi-material load sensor to check flexibility
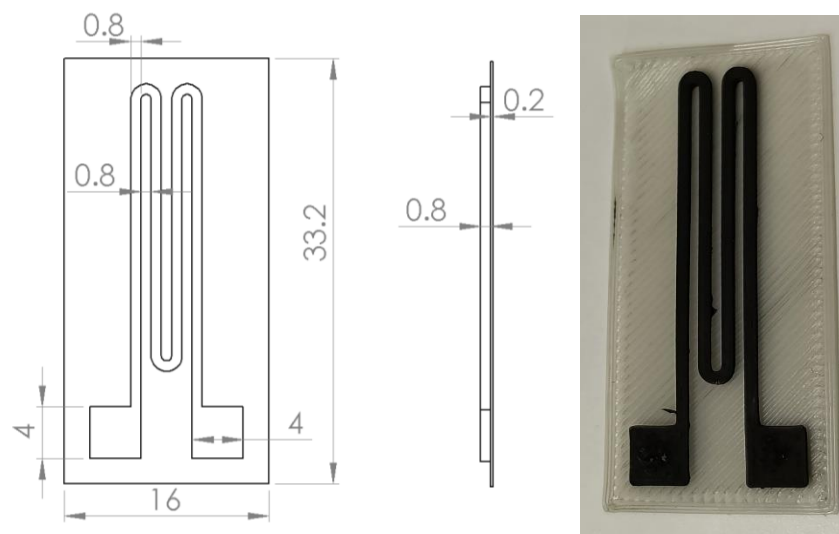
Fig.27. Preliminary design of a 3D printed load sensor with two turns of conductive PLA

Design of the zigzag structured multi-layered component was also an iterative process. The first few designs were printed, just to check the maximum flexibility of multi-material prints. Figure 27 shows the first 3D printing of zigzag structured load sensor with two turns of strain gauge. Base layer printed with BioFlex filament, and on top of it, a serpentine structured conductive layer. Conductive layer was printed with ProtoPasta conductive PLA with nozzle temperature while printing was 225 °C and nozzle diameter of 0.8 mm was used. The layer height was 0.2 mm SPEED while slicing the model. However, the flexibility of the printed component was limited to 35° to 40° angles. The reason for less flexibility was that the ProtoPasta conductive PLA filament has carbon black in molecular structure which results in a stiffer print. In addition, the thickness of the conductive layer was comparatively greater, which again leads to a stiffer structure. The conductive structure got broken into two after a try to bend more than 43° angle.
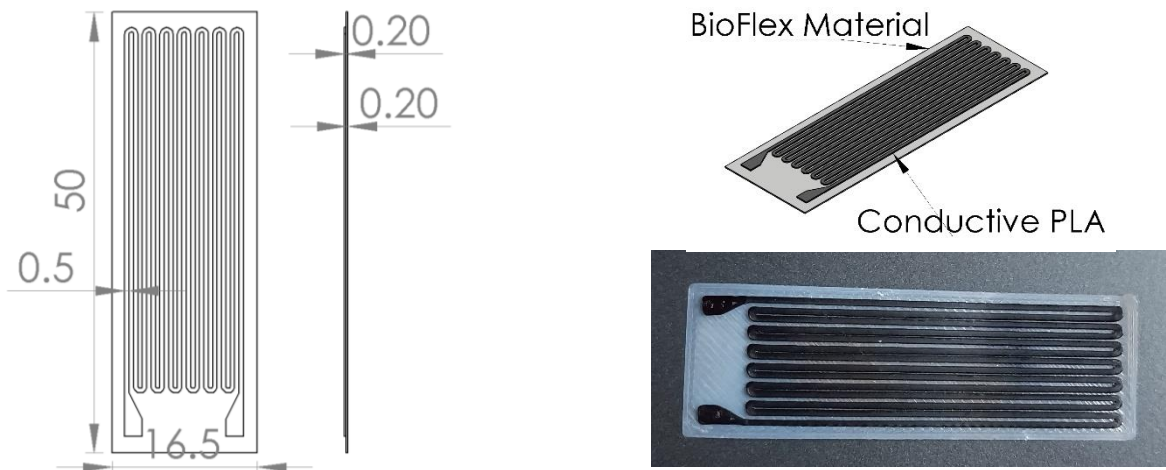
Fig.28. Second design of load sensor with seven turns of conductive PLA

The Figure 28 represents the second design iteration to test the maximum flexibility of the components, with only 0.2 mm of Bioflex substrate layer and 0.2 mm of printed conductive PLA. This component has greater flexibility due to its extremely thin design and single-layer printing. This component is capable of bending a full 360 degrees and rolling completely inside and outside around a 10 mm circular object.

3.2. Design of load sensor for perpendicular load

(a)   (b)   (c)

(d)   (e)
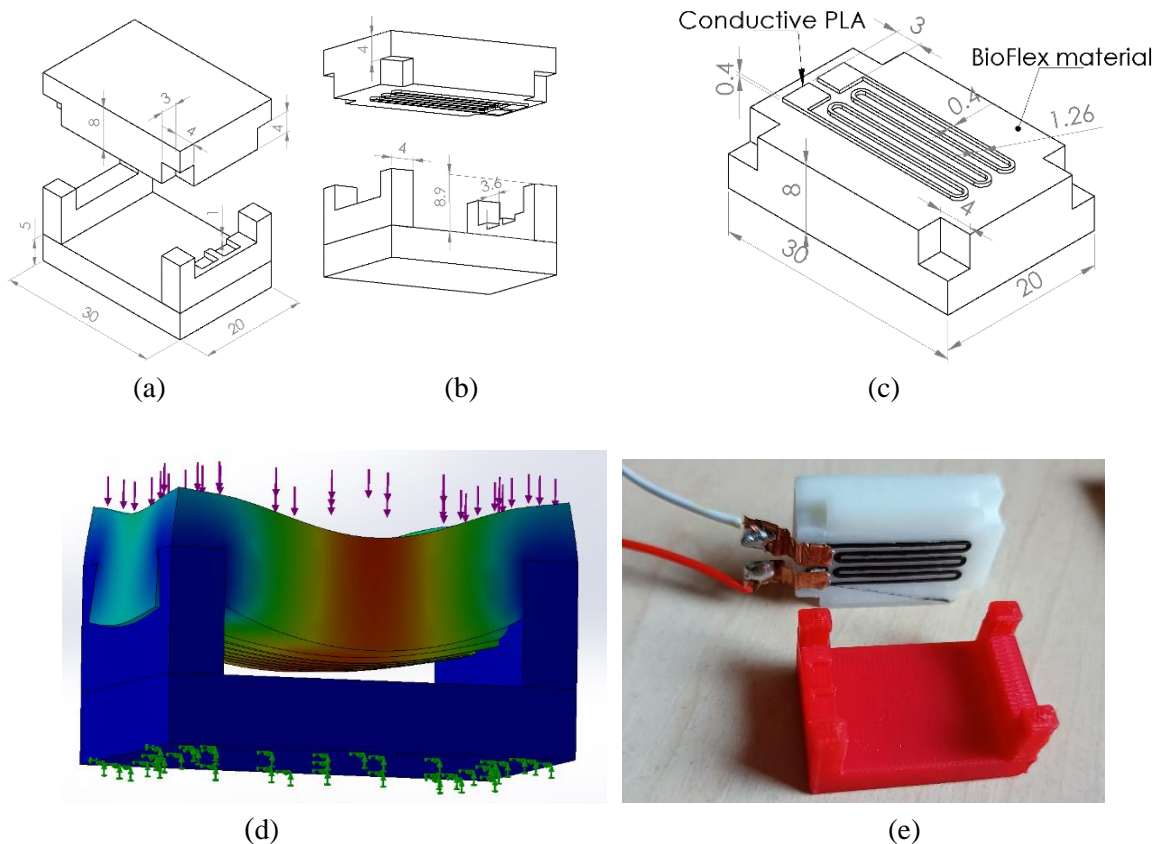
Fig.29. (a) and (b)assembly design of load sensor (c) CAD design of top having strain gauge (d) simulation of load sensor when load applied vertically downward (e) photo of printed load sensor

During this part the research, a load sensor has been designed for the load perpendicular to plane of the conductive strain gauge structured layer. The design model has base and a top (two-part structure)

33

as shown in Figure 29. Among the parts, the base was printed with a generic red PLA filament, the structure of the upper part was printed with BioFlex filament, and the conductive strain gauge was printed with ProtoPasta conductive filament. The printing temperature was 220 $^{\circ}$C for the base and cooling fan was on during the printing, whereas printing temperature was 230 $^{\circ}$C for BioFlex as well as conductive PLA and cooling fan was off. Figure 29 (d) shows that the simulation of the maximum displacement at the middle of the top portion of the sensor when an external force is applied. For that simulation, the base was fixed to the ground and an external force was applied vertically downward. Figure 29 (e) shows the actual picture of the printed sensor.

Two slots were designed inside the wall of the base for electrical connections. Since direct soldering is not possible on the pads of a 3D printed strain gauge, silver paste and copper strips were applied. The silver paste acted as an adhesive between the copper strips and pads of the 3D printed strain gauge, and then the wires were soldered to the copper strips. The sensor was assembled with all components, but there was no resistance value. After analysis of contact resistance near the strain gauge pads, it requires very tight contact between copper strips and pads of 3D printed strain gauge. The sensor gave an initial resistance value when the additional force was applied closer to the electrical connection. The looseness of the connections leads to high contact resistance values and the initial measured resistance of this sensor was around 6.8 MΩ. Furthermore, the main downside of this sensor is that it requires an initial force to ensure tight connection, if the connections were disturbed and no signal output from the sensor.

3.3. Design of load sensor for parallel load
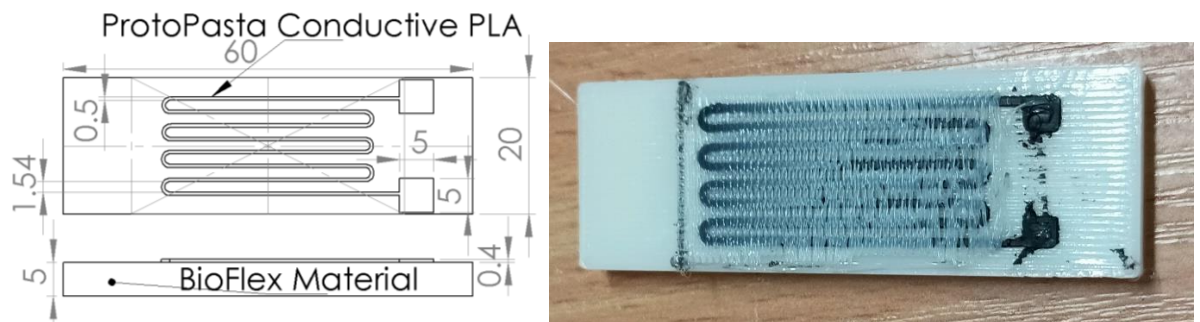
Fig.30. CAD design load sensor for load parallel to plane of strain gauge and actual 3D printed sensor

A new design model for parallel applied load to the plane of a 3D printed strain gauge has been developed after a thorough examination of previous research. For this type of sensor, BioFlex filament substrates with dimensions of 60 x 20 x 5 mm and strain gauge strips with a thickness of 0.5 mm were printed as shown in the figure. The connection pads of a 3D printed strain gauge were designed to be 5 x 5 mm. Throughout the printing structure, the infill density was 100 percent, and 0.4 nozzle was used. Printing speed was 10 mm/s for the first layer, 30 mm/s for infill patterns, and 10 mm/s for the conductive filament. The first layer printing temperature was 230 °C, followed by 225 °C for an infill pattern and conductive filament. The BioFlex filament was used to print a very thin, 0.2 mm layer on top of the sensor in order to increase its adhesion to the base.
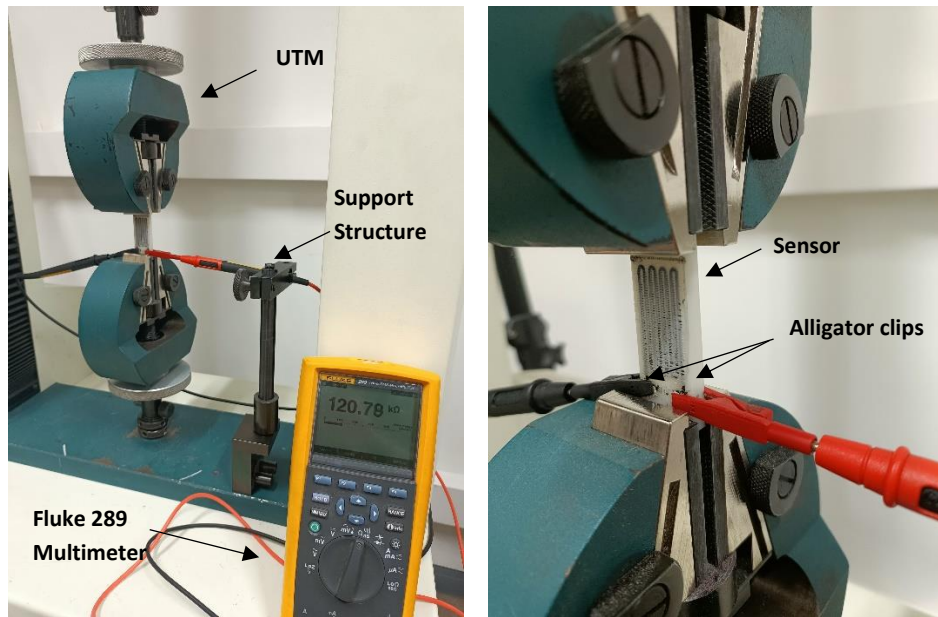
Fig.31. Experimental setup to determine piezoresistive sensitivity

To measure the initial resistance, silver paste was applied to the pads of a 3D printed strain gauge, and the resistance was measured using a Fluke 289 true RMS multimeter with alligator clips directly connected to the silver paste and the pads of printed strain gauge. The load sensor was placed between the upper and lower jaws of UTM and a 25KN load cell was used for the test. Load was applied with steps of 5N, starting from 0 N to 70 N and resistance value was measured.
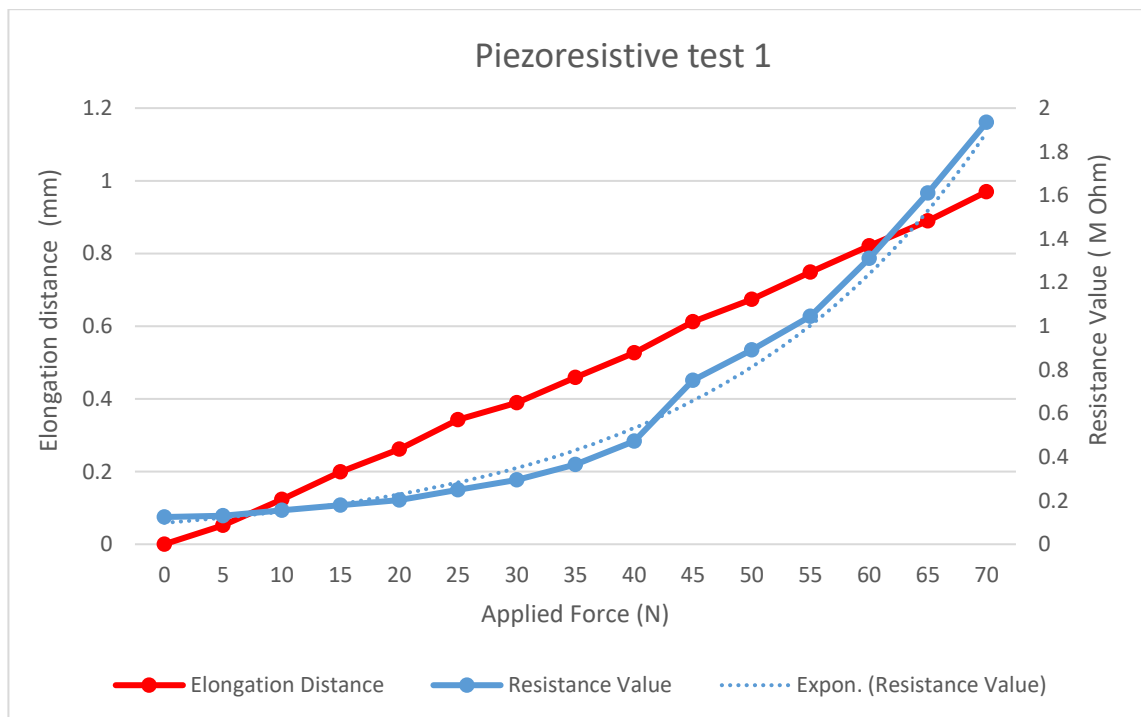
Fig.32. Experimental result of piezoresistive test 1
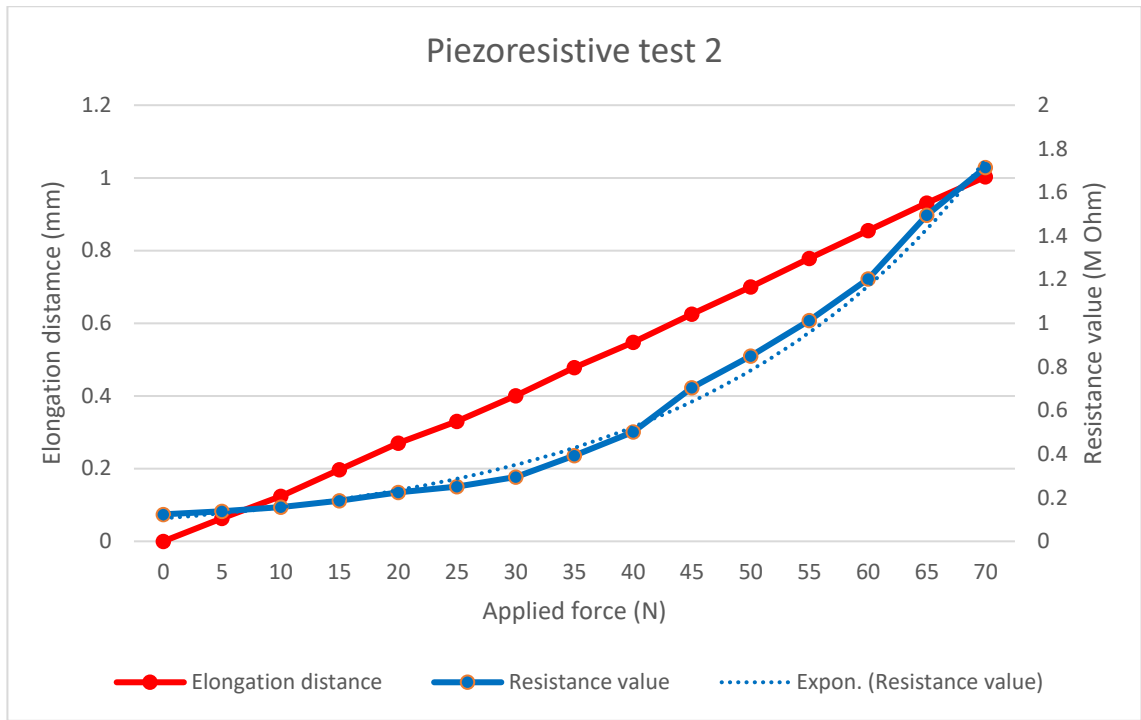
Fig.33. Experimental result of piezoresistive test 2

The piezoresistive test results are displayed in the above Figure 32 and Figure 33, where the x axis represents the applied load (N), the first y axis represents sensor elongation (mm), and the second y axis represents the resistance values during the test (MΩ). Both tests were carried out within an elastic limit of the load sensor. The slope of the trend lines of resistance values when applied load is parallel to the plane of a 3D printed strain gauge increases exponentially.

3.4. Circuit design for post processing

Experimental testing of the piezoresistive load sensor shows that the internal resistance value of the sensor was around 120 kΩ without any load and it increases to 2 MΩ when 70 N force was applied. However, the resistance value was around 1 MΩ when the applied force was 55 N. Taking into account the safety factor of the load sensor and the exponential characteristics of load sensor during higher load, a decision has been made to develop a circuit up to 1 M Ω internal resistance. Figure 34 shows the developed circuit for measurement of applied load using Proteus circuit simulator. The circuit consists of four parts, the first one is the load sensor itself. For simulation in the software variable resistor having maximum resistor 1 MΩ was used. The second part of circuit has a Wheatstone bridge, where R2 = R3 = R4 = 50 KΩ has been considered. The load sensor was connected to the bridge as a fourth resistor and a 50 V supply was applied to the bridge. The third part of a circuit consists of a differential amplifier. One of the popular operational amplifiers (op amp) 741 was used in the simulation due to its excellent availability.

The output voltage for the differential amplifier can be calculated as,

$$Vout = VB \left(\frac{RG}{RB+RG} \right) \left(\frac{RA+RF}{RA} \right) - VA \left(\frac{RF}{RA} \right) , \qquad \qquad \dots (2)$$

where Vout is the output voltage of op amp, VA and VB are the input voltages to op amp and RF is the feedback resistor. Resistor values were chosen as RA = RB = RG = RF = 10KΩ, the only condition was that all four values should be equal, which results into $Vout = VB - VA$ and VCC value for op amp was +12V for +VCC and -12V for – VCC.
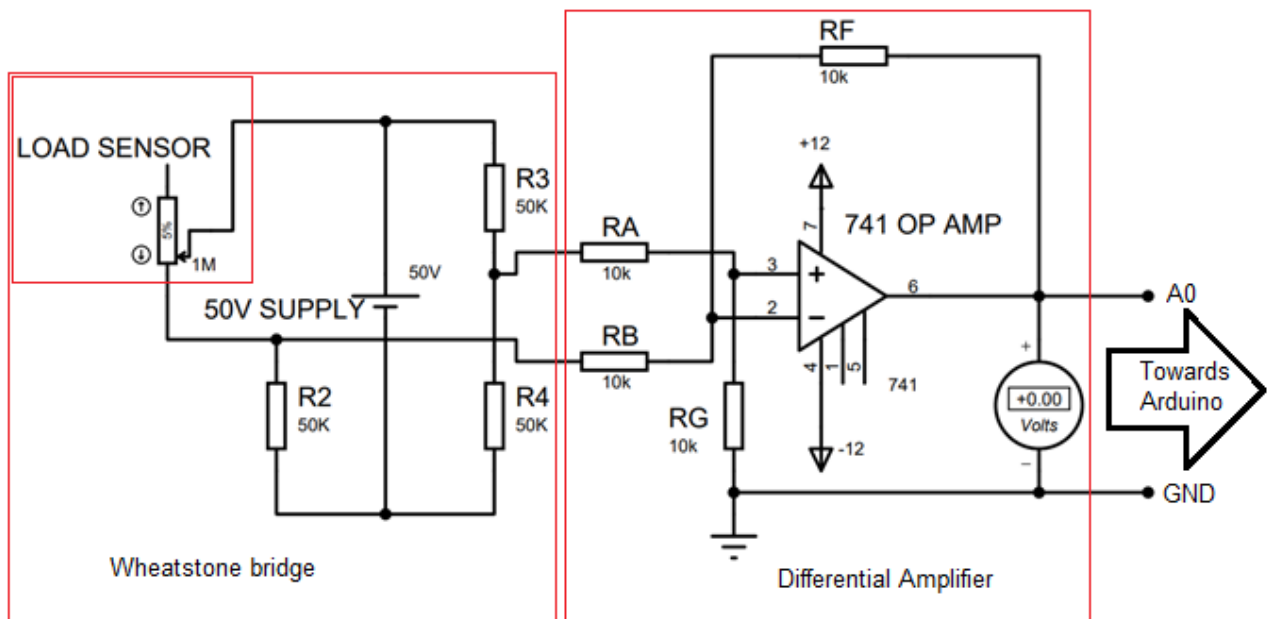
Fig.34. Developed circuit for measurement of applied load

For simulation of the circuit, DC voltmeter was used for measurement of the output voltage. Simulation using Proteus software shows that the output voltage is equal to 0V when the variable resistor was in 5 % stage and 4.89 V when 100% stage 1 MΩ. Voltages below 5V could easily be measured by Arduino analog input pins. Figure 35 shows a 3D visualisation of the printed circuit board (PCB) design.
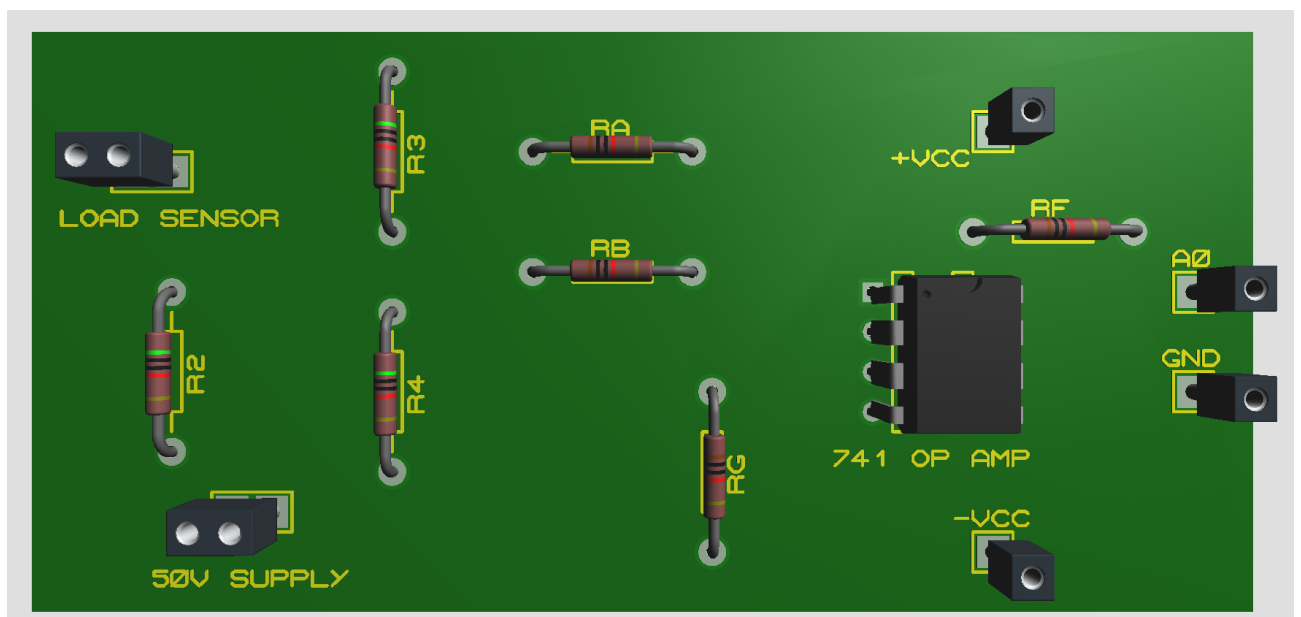
Fig.35. E-CAD model of the proposed circuit

In the fourth part of a circuit, the output terminals of the differential amplifier were connected to an analog input A0 pin of Arduino and GND, which is ground of Arduino. Arduino uses analog signal processing and gives values up to 1023, so the voltage output can be calibrated by multiplying 5/1023. After converting the resistance change of a piezoresistive load sensor into a digital output form of voltage change, it can be used directly for load sensor calibration.

4. Estimation of the cost required for load sensor development

This section of the research focusses primarily on the cost of load sensor development and testing. Considering that the research was conducted within an industry's R&D department, including the costs of the 3D printer, filaments, and UTM for testing.

Table 6. Cost of materials, tools and machine were used in this project

No.	Machine/ Material/ Tool	Price in EUR (including shipping)
1.	Prusa i3 MK3s 3D printer	1200
2.	Bondtech LGX extruder	150
3.	Generic PLA filament	25/ kg = 0.025 EUR/g
4.	BioFlex filament	40 for 250 grams = 0.16 EUR/g
5.	Protopasta Conductive PLA filament	70 for 500 grams = 0.14 EUR/g
6.	Nylon FX256 filament	75 / kg = 0.075 EUR/g
7.	ColorFabb XT-CF20 filament	58 / kg = 0.058 EUR/g
8.	3D printer maintenance tools	200
9.	Tinius Olsen H25KT UTM with ADLINK EOS-1200 Embedded Vision System and Monitor	14000

Machine hourly rate of a 3D printer

$$MHR = \frac{\text{Depreciation cost+Occupancy cost+Energy cost+Employee cost+Maintenance cost+Additional cost}}{\text{Machine working time}} \qquad \text{…(3)}$$

- Prusa i3 MK3s printer can be used 24 hours during business days that is why the machine working time can be considered as 6240 hours per year
- Occupancy cost = Space cost rate X 12 months X space required
  Considering the space cost rate 7 EUR and space required for 3D printer with operator = 1 m^2
  Occupancy cost = 7 X 12 X 1 = 84 RUR per year
- Cost of depreciation $= \dfrac{1200+200+150+250}{10} = 180$ EUR per year
- For the calculation of the energy cost, considering 90% efficiency, Power required for a 3D printer = 250 W, and energy price per kWh = 0.14 EUR. So, energy price = 196.56 EUR, after approximation the energy price would be 200 EUR per year for the 3D printer.
- For the calculation of employee costs, the 8-hour shift for all five business days and the hourly salary for the employee were set as 12 EUR/hour. However, 3D printing does not require complete presence of an employee, attention needed only for the first few layers, and the end of print. Periodic observation can be enough. So, considering 35 % for calculation. So, the employee cost can be reduced to 8700 EUR per year.

Machine hourly rate (MHR$_{printer}$) $= \dfrac{180+ 84+ 200+ 8700}{6240} = 1.47$ EUR.

Machine hourly rate for universal testing machine

- Similar to 3D printer, UTM also can be used 24 hours for all business days, so the machine working time would be the same 6240 hours per year for UTM as well.
- Considering the space cost rate 7 EUR and space required for the UTM with operator = 5 m^2, so the occupancy cost = 7 X 12 X 5 = 420 EUR per year.

- Cost of depreciation $= \dfrac{14000}{10} = 1400$ EUR per year.
- Energy cost calculations, considering 90% efficiency, power required for printer = 3.5 kW, and energy price per kWh = 0.14 EUR. So, energy price = 0.9 X 3.5 X 0.14 X 6240 = 2751.84 EUR, after approximation the energy price would be 2750 EUR per year for UTM.
- For the calculation of employee costs, the 8-hour shift of employee for all five business days and the hourly salary for an employee were settled as 12 EUR/hour. UTM requires full attention during any testing, so the employee cost will be 24960 EUR per year.
- Maintenance costs and other miscellaneous costs of 400 EUR per year taken into consideration

Machine hourly rate (MHR$_{UTM}$) $= \dfrac{420+2750+1400+24960+400}{6240} = 4.8$ EUR.

Material and testing cost

As this research study uses a standard single extruder 3D printer, one of the limitations of using a single extruder 3D printer is that every nozzle changes and filament change requires almost 2-3 g of purging of the filament, which can be saved from being wasted just by using multi-extruder printer. For material calculations, 2 g of additional material was considered for each filament change.

- For the tensile test specimens, 22 g of filament for two samples and 50 min of printing time; therefore, the manufacturing cost was 1.78 EUR and 40 min of testing using UTM, which means that the testing cost was 3.2 EUR and the total cost 1.78 + 3.2 = 4.98 EUR
- The printing time for the shear test fixture with Nylon 256 filament took around 1.5 hrs and 17 g of filament each, so the cost was 17.78 EUR for all five prints.
- To print the shear test fixture with ColorFabb XT-CF 20 filament, 18 g filament was used for the first design and 41 g filament was used for the second design; however, the printing time for the first design was 80 minutes and the printing time for the second design was 3 hours and 20 minutes. Therefore, the manufacturing costs for the first and second fixture designs were 3 EUR and 7.28 EUR, respectively.
- For single shear test specimens, on average 5.8 g of generic PLA filament, almost 2.8 g of BioFlex filament and 2 g of ProtoPasta conductive PLA were used. Printing time for the single shear test specimen was around 24 minutes on average, which means 1.46 EUR per specimen.
- For shear the testing using UTM, testing time depends on number of specimens in a batch. In this research, a batch of two specimens took around 35 minutes, whereas a batch of four specimens took around 50-55 minutes. So, on average 15.6 minutes per specimen which cost 1.25 EUR per specimen to test
- For a load sensor where the applied force direction was perpendicular to the plane of the conductive layer, 9 g of Bioflex filament and 3 g of PLA filament were used. The base of the sensor was printed in 25 minutes and the top in 75 minutes, resulting in a manufacturing cost of 4.3 EUR.
- 13 g of BioFlex filament and 4 g of conductive PLA were used to fabricate a load sensor of a parallel load. Because the printing time was 1.60 hours and the manufacturing cost was 4.91 EUR, and since the UTM testing time was 50 minutes, the testing cost was 4 EUR.
- In comparison to similar tensometric beams on the market, whose price ranges from 5.7 to 26.6 EUR based on the applied load, the fabricated load sensor demonstrates the advantages of both load and flex sensors, with greater customization being a major highlight of design.

Conclusions

The project perfectly demonstrates the following conclusion, which is based on the four completed tasks.

1. CAD models for 3D printing of a serpentine structured electroconductive PLA filament on top of BioFlex substrate filament were designed using SolidWorks software. In total, nine different CAD designs including fixtures and specimens were established for mechanical strength measurement, and five different CAD models were developed for piezoresistive testing of the load sensor. A suitable circuit was proposed for postprocessing of the results along with an e-CAD model of the circuit.

2. A novel experimental procedure with custom-designed test fixtures was developed to evaluate interlayer bonding strength rapidly and effectively, for 3D printed multi-layered components. According to this procedure, the low variation and the highest shear force required to remove the pillars of Protopasta conductive PLA from BioFlex material when the printing temperature was close to 230 ℃.

3. The multi-layered piezoresistive load sensor was fabricated using Prusa i3 MK3 single extruder 3D printer. The experimental test results showed an exponential increase in the internal resistance from 120 kΩ to 1.8 MΩ of the printed load sensor when a force ranging from 0 to 70 N was applied.

4. The estimated manufacturing cost required for the piezoresistive load sensor was 4.91 EUR, when the hourly rate of the Prusa i3 MK3 printer and UTM was 1.47 and 4.8 EUR respectively. Moreover, the developed 3D printed load sensors are highly customisable.

List of References

1. CHOUDHARY H, KUMAR H. A Review on Additive Manufactured Sensors. *Springer Link* [online]. MAPAN volume 36, pages 405–422. 2021. [viewed 20 September 2022]. Available from: https://doi.org/10.1007/s12647-020-00399-w

2. CHEN C, WANG X. Additive Manufacturing of Piezoelectric Materials. *Advanced Functional Materials* [online]. Volume 30, Issue 52. 2020 [viewed 20 September 2022]. Available from: https://doi.org/10.1002/adfm.202005141

3. LIU H, ZHANG H. 3D Printed Flexible Strain Sensors: From Printing to Devices and Signals. *Advance materials* [online]. Volume 33, Issue 8. 2021. [viewed 22 September 2022]. Available from: https://doi.org/10.1002/adma.202004782

4. XUE J, ZOU Y. Bioinspired sensor system for health care and human-machine interaction. *EcoMat* [online]. Volume 4, Issue 5, e12209. 2022 [viewed 23 September 2022]. Available from: https://doi.org/10.1002/eom2.12209

5. KWON S, KIM S. Direct 3D Printing of Graphene Nanoplatelet/Silver Nanoparticle-Based Nanocomposites for Multiaxial Piezoresistive Sensor Applications. *Advanced materials technology* [online]. Volume 4, Issue 2. 2019. [viewed 7 October 2022]. Available from: https://doi.org/10.1002/admt.201800500

6. NASSAR H, NAVARAJ W. Multi-Material 3D Printed Bendable Smart Sensing Structures. *IEEE Xplore* [online]. INSPEC Accession Number: 18348594. 2018. [viewed 8 October 2022]. Available from: https://doi.org/10.1109/ICSENS.2018.8589625

7. MUTH J. Embedded 3D printing of strain sensors within highly stretchable elastomers. *Advanced Materials* [online]. volume 26. 2014. [viewed 8 October 2022]. Available from: https://doi.org/10.1002/adma.201400334

8. CHANG Y, WANG K. A facile method for integrating direct-write devices into three-dimensional printed parts. *IOPscience* [online]. Smart Materials and Structures 24 065008 (8pp). 2015. [viewed 8 October 2022]. Available from: https://doi.org/10.1088/0964-1726/24/6/065008

9. KOUCHAKZADEH, S. Simulation of piezo-resistance and deformation behaviour of a flexible 3D printed sensor considering the nonlinear mechanical behaviour of materials. *Sensors and Actuators A: Physical* [online]. volume 332, page 113214. 2021. [viewed 9 October 2022]. Available from: https://doi.org/10.1016/j.sna.2021.113214

10. MILETI I, CORTESE L. Reproducibility and embedding effects on static performance of 3D printed strain gauges. *IEEE International Workshop on Metrology for Industry 4.0 and IoT* [online]. Page 499-504. 2021. [viewed 10 October 2022]. Available from: https://doi.org/10.1109/MetroInd4.0IoT51437.2021.9488430

11. ELGENRIDY K, JACKSON M. Directly Printable Flexible Strain Sensors for Bending and Contact Feedback of Soft Actuators. *Frontiers in Robotics and AI* [online]. 2019. [viewed 12 October 2022]. Available from: https://doi.org/10.3389/frobt.2018.00002

12. LAZARUS N, BEDAIR S. Creating 3D printed sensor systems with conductive composites. *IOPscience* [online]. Smart Materials and Structures 30 015020. 2021. [viewed 12 October 2022]. Available from: https://doi.org/10.1088/1361-665X/abcbe2

13. STANO G, NISIO A, RANGOLIA M. Fused filament fabrication of commercial conductive filaments: experimental study on the process parameters aimed at the minimization, repeatability and thermal characterization of electrical resistance. *SpringerLink* [online]. 111, pages 2971–

2986. 2020. [viewed 15 October 2022]. Available from: https://doi.org/10.1007/s00170-020-06318-2

14. PRUSA RESEARCH. Fiberthree F3 PA-CF Pro technical datasheet [online]. 2020. Available from: https://www.prusa3d.com/file/133/technical-data-sheet.pdf

15. PRUSA RESEARCH. ColorFabb XT-CF20 technical datasheet [online]. 2017. Available from: https://www.prusa3d.com/file/76328/technical-data-sheet.pdf

16. DSM. Novamid® id1030 cf10 technical data sheet. [online]. 2018. Available from: https://www.dsm.com/content/dam/dsm/additive-manufacturing/en_US/documents/novamid-id1030-cf10-leaflet.pdf

17. LUVOCOM. 3F PAHT CF 9891 BK datasheet [online]. 2020. Available from: https://www.crea3d.com/en/index.php?controller=attachment&id_attachment=523

18. BASF. Ultrafuse PAHT CF15 technical datasheet [online]. 2019. Available from: https://www.crea3d.com/en/index.php?controller=attachment&id_attachment=157

19. JABIL. PA 4535 CF technical datasheet [online]. 2020. Available from: https://www.jabil.com/dam/jcr:1698a0a2-f2de-460c-ba53-aef6409530a3/Jabil%20PA%204535%20CF_TDS_DIGITAL_04.pdf

20. OWENS CORNING XSTRAND™ GF30-PA6 technical datasheet [online]. 2018. Available from: https://www.crea3d.com/en/index.php?controller=attachment&id_ attachment=138

21. 3DXTECH. FibreX™ PP+GF30 technical datasheet [online]. 2022. Available from: https://www.3dxtech.com/wp-content/uploads/2021/04/GF_PP_v1.pdf

22. PROTOPASTA. CDP1xxxx Safety Data Sheet [online]. 2018. Available from: https://cdn.shopify.com/s/files/1/0717/9095/files/CFP1xxxx_SDS.pdf?199260627289763

23. FILOALFA. Alphaohm technical datasheet [online]. 2019. Available from: https://www.filoalfa3d.com/img/cms/MSDS%20&%20TDS/TDS%20ALFAOHM%20Sept,%202019.pdf

24. FIBER FORCE. technical data sheet: Nylforce Carbon Fiber. [online]. 2019. Available from: https://cdn-3d.niceshops.com/upload/file/TDS_NYLFORCE-CF-Fiber-Force-2017.pdf

25. NINJATEK. Technical Specifications: Eel 3D Printing Filament. [online]. 2018. Available from: https://ninjatek.com/wp-content/uploads/Eel-TDS.pdf

26. RAISE3D. Technical Data Sheet: Premium TPU-95A [online]. 2021. Available from: https://s1.raise3d.com/2021/06/Raise3D-Premium-TPU95A_TDS_V1.pdf

27. FILOALFA. Technical Data Sheet: BioFlex [online]. 2020. Available from: https://www.filoalfa3d.com/gb/content/12-bioflex

28. BASF. Ultrafuse TPU 85A Technical Data Sheet [online]. 2019. Available from: https://www.crea3d.com/en/index.php?controller=attachment&id_attachment=301

29. KIMYA. TPU-92A 3D Filament Technical datasheet [online]. 2021. Available from: https://www.crea3d.com/en/index.php?controller=attachment&id_attachment=301

30. BCN3D TPU 98A Technical data sheet [online]. 2018. Available from: https://www.crea3d.com/en/index.php?controller=attachment&id_attachment=368

31. MULLAVEETTIL F, DAUKSEVICIUS R. Fused filament fabrication and mechanical performance of PVDF-based specialty thermoplastics. *International Journal of Advanced Manufacturing Technology* [online]. P. 3267–3280. 2021. [viewed 11 November 2022]. Available from: https://doi.org/10.1007/s00170-021-07887-6

Recommendations

1. For load sensor calibration, integration of operational amplifiers and differential amplifier circuits, it is possible to calculate the unknown applied force from the resistance change.

2. More design customisation, higher dimensional stability, and less wastage of printing filaments with reduced printing time can be achieved using a multi-extruder 3D printer.

3. Using multi-material 3D printing, a fully 3D-printed tactile sensor can be developed. In addition, a robotic end effector with built-in sensors can be 3D printed jointly during part fabrication.

4. Highest customizability in sensor design paved the way to use multi-material 3D printing in smart prosthetic design, smart garments.
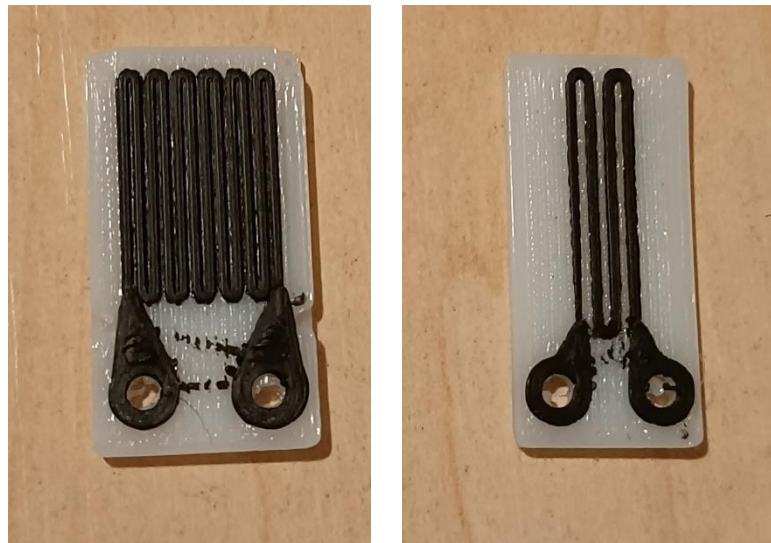
Appendix 1. Graphical representation of specimens with high coefficient of variation
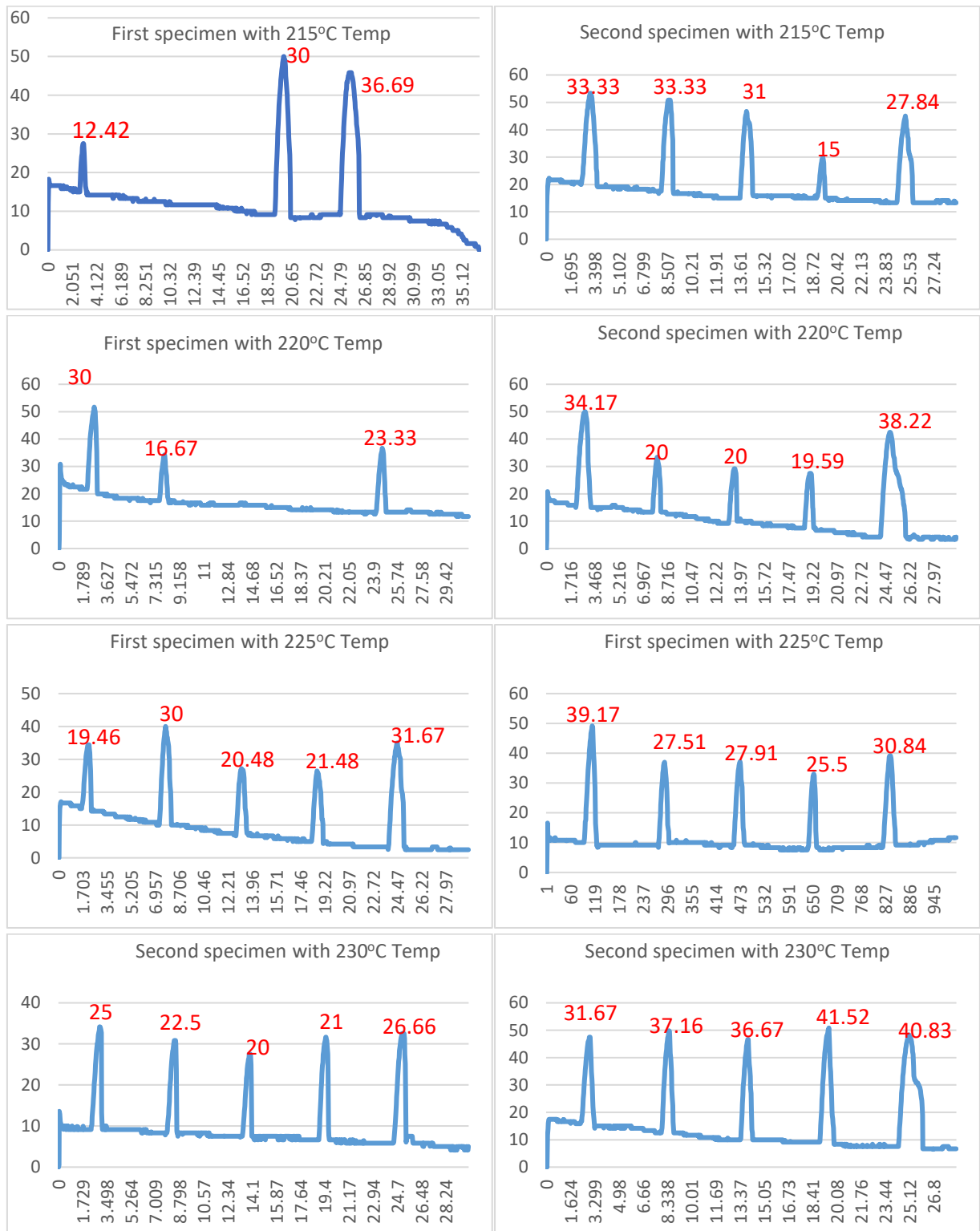

These graphs represent shear test values that have a higher coefficient of variation among test specimens with pillars.

Appendix 2. Another failed structure of load sensor for perpendicular load

These designs of 3D printed load sensor were related to the load perpendicular to plane of strain gauge. The interim plan was to overcome the loose contacts between copper strips and the 3D printed conductive filament. The CAD model of the top part was designed in such a way that a 3 mm hole was planned to use nut bolts and washers to provide tightness in a contact. However, the compressibility of BioFlex results in slippage. Therefore, the printed samples do not show any output.

Appendix 3. Simulation results of the proposed circuit for calibration of load sensor.
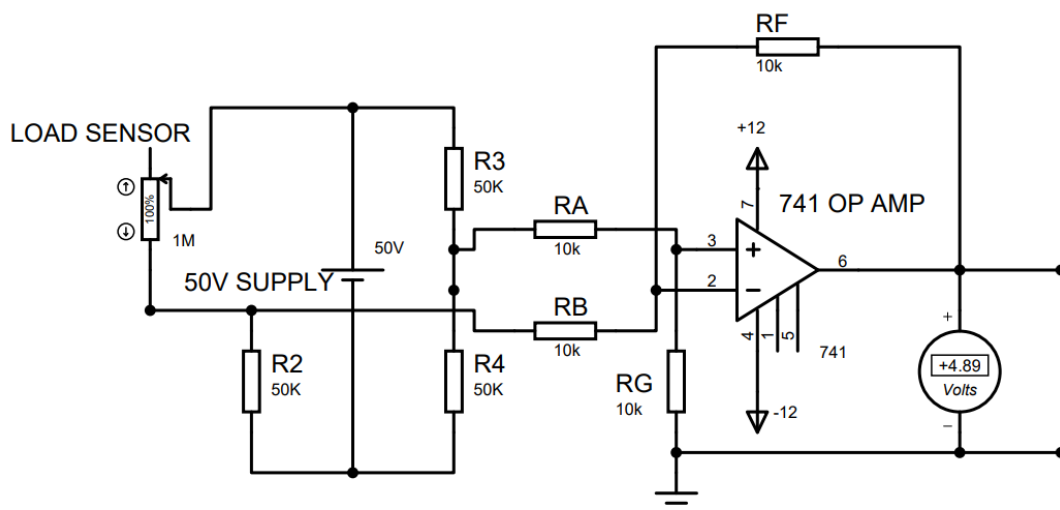
The simulation shows the output voltage as 4.89V when the internal resistance of the load sensor is equal to 1 MΩ. The output voltage of 0-5V can be directly converted into digital format using analog pins of Arduino.